

# **M<sub>12</sub>L<sub>24</sub> nanospheres as supramolecular templates for the controlled synthesis of Ir-nanoclusters and their use in the chemo-selective hydrogenation of nitro styrene**

**Lotte L. Metz<sup>a)</sup>, Rens Ham<sup>a)</sup>, Eduard O. Bobylev<sup>a)</sup>, Kelly J. H. Brouwer<sup>b)</sup>, Alfons van Blaaderen<sup>b)</sup>, Rim C. J. van de Poll<sup>c)</sup>, Victor, R. Drozhzhin<sup>c)</sup>, Emiel J.M. Hensen<sup>c)</sup>, Joost N. H. Reek\*<sup>a)</sup>**

<sup>a)</sup> Van 't Hoff Institute for Molecular Sciences, University of Amsterdam, 1098 Amsterdam, The Netherlands.

<sup>b)</sup> Soft Condensed Matter, Debye Institute for Nanomaterials Science, Utrecht University, Princetonplein 1, 3584 CC, Utrecht, The Netherlands

<sup>c)</sup> Department of Chemical Engineering and Chemistry, Eindhoven University of Technology, 5600 MB Eindhoven, The Netherlands

## CONTENTS

General information .....	3
Synthesis of the <b>Ir-s</b> metal precursor .....	4
Synthesis of <b>Ir-p</b> metal precursor .....	6
NMR spectra of synthesized metal complexes .....	8
Synthesis G-Sphere building block: <b>GuaniBB</b> .....	16
NMR spectra of <b>GuaniBB</b> and <b>S8</b> ) .....	18
Synthesis and characterization of <b>G-sphere</b> (M <sub>12</sub> L <sub>24</sub> ) .....	19
NMR and MS spectra of <b>Pt-G-sphere</b> and <b>Pd-G-sphere</b> .....	22
Binding experiments ( <sup>1</sup> H-NMR studies) .....	32
Binding <sup>1</sup> H-NMR titration experiment .....	36
MS-binding experiment .....	40
Nanocluster synthesis .....	47
TEM images of control groups .....	50
Catalysis: General procedure of the catalytic tests over time .....	53
Catalysis: General procedure of High-Pressure NMR experiments .....	54
X-ray photoelectron spectroscopy (XPS) .....	57
Presence of Silver impurities: .....	59
Experimental References .....	61

---

## General information

All reactions (unless stated otherwise) were performed under inert atmosphere using standard Schlenk techniques. CH<sub>3</sub>CN was dried by passage through purification columns and CD<sub>3</sub>CN was dried over finely powdered molsieves both were degassed prior to use. CH<sub>2</sub>Cl<sub>2</sub> was dried by distillation over CaH<sub>2</sub> and THF through distillation over Na. Dry N,N-Dimethylformamide (DMF) with AcroSeal was purchased from Thermo Fischer Scientific Mesitylimidazole<sup>1</sup>, 1-Mesityl-3-(4-sulfonatopropyl)imidazolium (**S1**)<sup>2</sup>, 1-mesityl-3-propyl-1H-imidazol-3-ium bromide (**S2**)<sup>3</sup>, **MethoxyBB**<sup>4</sup>, Pd(CH<sub>3</sub>CN)<sub>4</sub>(BF<sub>4</sub>)<sub>2</sub><sup>4,5</sup>, Pt(CH<sub>3</sub>CN)<sub>4</sub>(BF<sub>4</sub>)<sub>2</sub><sup>4,5</sup> and (**S6**)<sup>6</sup> were synthesized according to literature procedures. All other reagents were purchased from commercial suppliers (Sigma-Aldrich, Fluorochem, STREM and Thermo Fischer Scientific) and used without further purification unless stated otherwise. The silica gel used for column chromatography was Macherey-Nagel, Silica 60, 0.04 – 0.063 mm). <sup>1</sup>H- and <sup>13</sup>CNMR spectra were recorded on the following instruments Bruker DRX 500, AMX 400, DRX 300 or AMX 300 spectrometer, with chemical shifts reported in ppm relative to TMS by reference to the relevant solvent residual signal.<sup>7</sup> 2D-DOSY NMR spectra were recorded on a Bruker DRX 300 at 25°C. GC-MS analysis was performed on a Shimadzu GCMS-QP2020 SE gas chromatograph mass spectrometer using the FID as detector and SH-Rtx-5 Amine column (30.0 m length, 0.25 µm internal diameter, 0.25 µm film thickness).

Cryospray-ionization MS (CSI-MS) and electrospray ionization (ESI-MS) mass spectra were measured on a HR-ToF Bruker Daltonik GmbH (Bremen, Germany) Impact II, an ESI-ToF MS capable of resolution of at least 40000 FWHM, which was coupled to a Bruker cryo-spray unit. Detection was in positive-ion mode and the source voltage was between 4 and 6 kV. The sample was introduced with a syringe pump at a flow rate of 18 µl/hr. The drying gas (N<sub>2</sub>) was held at 60°C or -35°C and the spray gas was held at 55°C or -40°C. The machine was calibrated prior to every experiment via direct infusion of a TFA-Na solution, which provided a m/z range of singly charged peaks up to 3500 Da in both ion modes. Software acquisition Compass 2.0 for Otof series. Software processing m-mass. The XPS spectra were recorded on a ThermoFischer Thermo Scientific K-Alpha X-ray Photoelectron Spectrometer with an Al Kα (1486.6 eV) source. The energy scale was calibrated by setting the C 1s of the carbon support to a binding of 284.8 eV.

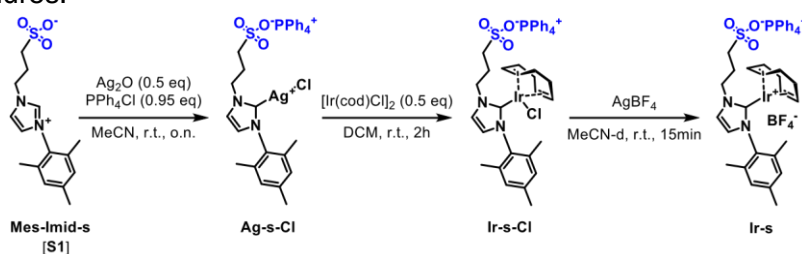
The TEM samples were prepared by direct dilution of particle mixture (100x, 86 µM in CH<sub>3</sub>CN and dropcasting onto a TEM grid (carbon film only on 200

mesh, Copper (Pure-C, 15-25 nm) used a purchased from Ted Pella). The TEM images were recorded on the FEI Tecnai 20 (type Sphera) operated with a LaB6 filament at 200 kV with a bottom-mounted CETA II 4k x 4k CMOS camera.

The HAADF-STEM-EDX measurements were measured on the Thermo Fisher Scientific Talos F200X TEM equipped with a field emission gun operated at 200 kV.

## Synthesis of the Ir-s metal precursor

Synthesis procedures of **Ag-s-Cl** and **Ir-s-Cl** are based on modified literature procedures.<sup>2,8,9</sup>



## Synthesis of **Ag-s-Cl**

All solids: **Mes-Imid-s (S1)** (0.420 g, 1.362 mmol 1 eq), **PPh<sub>4</sub>Cl** (0.484 g, 1.294 mmol 0.95 eq) and **Ag<sub>2</sub>O** (0.158 g, 0.681 mmol, 0.5 eq) were weighted and added to a flame dried flask. 24 ml acetonitrile is added, the mixture is excluded from light and stirred overnight at room temperature. The next day, the grey suspension is filtered over celite, yielding a colourless solution. The solvents are removed in vacuo, yielding **Ag-s-Cl** as a white foamy solid. (1.001 g 93% yield) <sup>1</sup>H NMR (400 MHz, CD<sub>2</sub>Cl<sub>2</sub>) δ 7.96 - 7.88 (m, 4H), 7.80 - 7.72 (m, 8H), 7.67 - 7.58 (m, 8.5H), 7.54 (s, 0.5H), 7.00 (s, 2H), 6.89 (d, *J* = 8.3 Hz, 1H), 4.46 (t, *J* = 6.6 Hz 1.3H), 4.16 (t, *J* = 6.8 Hz, 0.7H), 2.67 (t, *J* = 6.6 Hz 1.3H), 2.54 (t, *J* = 6.6 Hz 0.7H), 2.39 (s, 1H), 2.34 (s, 2H), 2.27 - 2.37 (m, 1.3H), 2.08 - 2.03 (m, 0.7H), 1.99 (s, 4H), 1.87 (s, 2H). <sup>13</sup>C NMR (126 MHz, CD<sub>2</sub>Cl<sub>2</sub>) δ 139.64, 136.08 (d, *J* = 3.0 Hz), 135.33, 134.80 (d, *J* = 10.3 Hz), 130.97 (d, *J* = 12.9 Hz), 129.96, 129.44, 123.21, 122.19, 117.87 (d, *J* = 89.7 Hz), 50.53, 47.54, 28.48, 21.17, 17.76, 17.61. ESI-(neg.)-MS-(TOF): [M - PPh<sub>4</sub>]<sup>-</sup> calculated for [C<sub>15</sub>H<sub>19</sub>AgClN<sub>2</sub>O<sub>3</sub>S]<sup>-</sup> *m/z* 450.9848 found *m/z* 450.9858. \*<sup>1</sup>H has splitting for the CH<sub>2</sub> and CH<sub>3</sub> peaks, this is a result of the compound being in equilibrium with its biscarbene form and restricted rotation. This was studied with T resolved <sup>1</sup>H-NMR (**Figure S35**). Nonetheless, this product can be used in the next step without any issue.

---

## Synthesis of **Ir-s-Cl**

The silver carbene (**Ag-s-Cl**) (200 mg, 0.253 mmol, 1 eq) and  $[\text{Ir}(\text{cod})\text{Cl}]_2$  (85.0 mg, 0.126 mmol, 0.5 eq) were weighted and separately placed into two flame dried schlenks. To both schlenks 5 ml of freshly distilled  $\text{CH}_2\text{Cl}_2$  is added. Then, the silver carbene is carefully added to the stirring Ir solution, resulting in immediate precipitation. The mixture is excluded from light and stirred for 2 hours at room temperature. Thereafter, the mixture is filtered over celite and solvents are removed in vacuo to yield (**Ir-s-Cl**) as an orange foamy solid (233.1 mg, 94% yield)  $^1\text{H}$  NMR (400 MHz,  $\text{CD}_3\text{CN}$ )  $\delta$  7.95 – 7.87 (m, 4H), 7.79 – 7.63 (m, 16), 7.41 (d,  $J = 2.0$  Hz, 1H) 7.03 (s, 1H), 6.98 (s, 1H), 6.88 (d,  $J = 2.0$  Hz, 1H), 5.03 – 4.85 (m, 1H), 4.45 – 4.24 (m, 2H), 4.16 – 4.02 (m, 1H), 3.07 (t,  $J = 7.0$  Hz, 1H), 2.79 (td,  $J = 7.4, 3.3$  Hz, 1H), 2.61 (t,  $J = 7.5$  Hz, 2H), 2.51 – 2.39 (m, 2H), 2.34 (s, 3H), 2.39 – 2.28 (m, 2H), 2.22 (s, 3H,  $\text{CH}_3$ ), 1.89 (s, 3H), 1.78 – 1.64 (m, 2H), 1.42 – 1.31 (m, 2H), 1.26 - 1.17 (m, 2H).  $^{13}\text{C}$  NMR (75 MHz,  $\text{CD}_3\text{CN}$ )  $\delta$  179.85, 139.63, 137.33, 136.39 (d,  $J = 3.0$  Hz), 136.00, 135.70 (d,  $J = 10.3$  Hz), 131.34 (d,  $J = 12.9$  Hz), 129.93, 129.07, 123.86, 122.91, 119.52 (d,  $J = 84.8$  Hz), 83.14, 81.67, 52.77, 52.01, 50.79, 49.30, 34.55, 33.70, 32.65, 29.79, 27.97, 21.12, 19.65, 18.08. ESI-(neg.)-MS(TOF):  $[\text{M} - \text{PPh}_4]^-$  calculated for  $[\text{C}_{23}\text{H}_{31}\text{ClIrN}_2\text{O}_3\text{S}]^-$  m/z 643.1379, found m/z 643.1301.

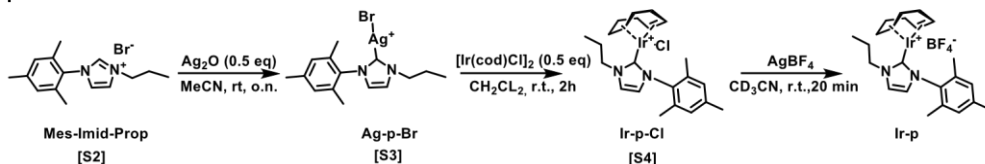
---

## Chloride abstraction to obtain **Ir-s-BF<sub>4</sub>**

An  $\text{AgBF}_4$  stock solution (0.160 ml, 0.380 M, 0.0607 mmol) in  $\text{CD}_3\text{CN}$  is added to a stirring solution of **Ir-s-Cl** in  $\text{CD}_3\text{CN}$  (0.075 M, 0.810 ml, 0.0607 mmol). The reaction immediately turns from an orange solution to an orange/white cloudy suspension with increasing amounts of precipitate. The mixture is excluded from light and stirred for 20 min at room temperature. Thereafter, the mixture is filtered through a syringe filter (0.45  $\mu\text{m}$ ) and used without further purification (qt.).  $^1\text{H}$ -NMR (300 MHz,  $\text{CD}_3\text{CN}$ )  $\delta$  ppm: 7.95 – 7.88 ppm (m, 4H), 7.77 – 7.64 ppm (m, 16H), 7.47 (d, 1H 2.0 Hz), 7.10 ppm (s, 1H), 7.06 (d, 1H, 2.0 Hz), 7.03 (s, 1H), 4.83 (m, 1H), 4.43 (m, 1H), 4.34 (m, 1H), 4.2 (m, 1H), 3.76 (m, 1H), 3.21 (m, 1H), 2.68 (t, 2H, 7.5 Hz), 2.39 (m 2H), 2.35 (s, 3H), 2.31 (m, 2H) 2.09 (s, 3H), 1.92 (s, 3H), 1.77 – 1.36 (m 6H).  $^{13}\text{C}$  NMR (126 MHz,  $\text{CD}_3\text{CN}$ )  $\delta$  174.45, 140.14, 136.62, 136.40 (d,  $J = 3.2$  Hz), 136.26, 135.70 (d,  $J = 10.2$  Hz), 131.33 (d,  $J = 13.0$  Hz), 130.08, 129.66, 125.15, 123.12, 118.93 (d,  $J = 89.6$  Hz), 83.15, 81.93, 66.37, 64.37, 50.94, 49.30, 34.22, 32.46, 30.35, 29.50, 28.34, 21.11, 18.65, 18.15 ESI-(Pos.)-MS-(TOF):  $[\text{M} (-\text{PPh}_4^+ - \text{BF}_4^-) + \text{H}]^+$  calculated for  $[\text{C}_{23}\text{H}_{32}\text{IrN}_2\text{O}_3\text{S}]^+$  m/z 609.1757, found m/z 609.1736.

## Synthesis of Ir-p metal precursor

**Ag-p-Br (S3)** and **Ir-p-Cl (S4)** were synthesized based on modified literature procedures<sup>10,11</sup>



## Synthesis of Ag-p-Br (S3)

1-mesityl-3-propyl-1H-imidazol-3-ium bromide (**S2**) (0.250 g, 0.808, 1 eq) and Ag<sub>2</sub>O (0.094, 0.404, 0.5 eq) were weighted and placed in a flame dried Schlenk flask and 5 ml of dry degassed CH<sub>3</sub>CN was added. The mixture was excluded from light and stirred overnight. The mixture was then filtered over a pad of celite, which was flushed with dichloromethane. The solvents were removed under vacuum to yield a white solid (318.6 mg, 0.766 mmol, 77% yield). <sup>1</sup>H NMR (300 MHz, CD<sub>2</sub>Cl<sub>2</sub>) δ 7.208 (d, *J* = 1.80 Hz, 1H), 7.008 (s, 2H), 6.986 (d, *J* = 1.80 Hz, 1H), 4.129 (t, *J* = 6.70 Hz, 2H), 2.357 (s, 3H), 1.972 (s, 6H), 1.891 (h, *J* = 7.35, 6.70 Hz, 2H), 0.931 (t, *J* = 7.35 Hz, 3H).

## Synthesis of Ir-p-Cl (S4)

**Ag-p-Br (S3)** (200 mg, 0.481 mmol, 1 eq) and [Ir(cod)Cl]<sub>2</sub> (42.5 mg, 0.063 mmol, 0.5 eq) were weighted and separately placed in two flame dried schlenks. Freshly distilled CH<sub>2</sub>Cl<sub>2</sub> was added to the Schlenks (3 ml to [Ir(cod)Cl]<sub>2</sub>, bright orange solution and 6 ml to **S3**, colourless solution). Then, the silver carbene is carefully added to the stirring Ir solution, resulting in immediate precipitation. The Schlenk is rinsed with an additional 3 ml CH<sub>2</sub>Cl<sub>2</sub> to transfer any leftover **S3** to the reaction mixture. The mixture is excluded from light and stirred for 2 hours at room temperature. Thereafter, the mixture is filtered over celite and solvents are removed in vacuo to yield **Ir-p-Cl (S4)** as an orange powder. <sup>1</sup>H NMR (400 MHz, CD<sub>3</sub>CN) δ 7.26 (d, *J* = 2.0 Hz, 1H), 6.04 (s, 1H), 6.98 (s, 1H), 6.92 (d, *J* = 2.0 Hz, 1H), 4.85 - 4.76 (m, 1H), 4.34 - 4.18 (m, 1H), 4.23 - 4.07 (m, 2H), 3.09 (td, *J* = 7.4, 2.3 Hz, 1H), 2.79 (td, *J* = 7.4, 3.3 Hz, 1H), 2.34 (s, 3H), 2.23 (s, 3H), 2.11 - 1.97 (m, 3H), 1.88 (s, 3H), 1.79 - 1.67 (m, 1H), 1.58 - 1.46 (m, 2H), 1.44 - 1.13 (m, 1H), 1.26 - 1.16 (m, 1H), 1.02 (t, *J* = 7.4 Hz, 3H) (~14% is Imidazolium salt) <sup>1</sup>H NMR (300 MHz, C<sub>6</sub>D<sub>6</sub>) δ 6.78 (s, 1H), 6.69 (s, 1H), 6.20 (d, *J* = 2.0 Hz, 1H), 5.93 (d, *J* = 2.0 Hz, 1H), 5.05 - 4.89 (m, 2H), 4.89 - 4.77 (m, 1H), 4.10 - 3.85 (m, 1H), 3.13 (t, *J* = 6.3 Hz, 1H), 2.92 (td, *J* = 7.3, 3.1 Hz, 1H), 2.56 (s, 3H), 2.30 - 2.16

(m, 1H), 2.12 (s, 3H), 2.10 - 1.99 (m, 1H), 1.94 - 1.77 (m, 2H), 1.73 (s, 3H), 1.66 - 1.48 (m, 5H), 1.38 - 1.23 (m, 1H), 0.79 (t,  $J = 7.4$  Hz, 3H). (no imidazolium peaks observed / 100% purity)  $^{13}\text{C}$  NMR (75 MHz,  $\text{C}_6\text{D}_6$ )  $\delta$  180.86, 138.55, 137.71, 134.42, 130.18, 129.99, 122.28, 120.41, 83.53, 83.41, 53.08, 52.93, 51.19, 50.42, 35.00, 33.31, 29.98, 29.41, 24.04, 21.01, 20.06, 11.29

ESI-(pos.)-MS-(TOF):  $[\text{M} - \text{Cl}]^+$  calculated for  $[\text{C}_{23}\text{H}_{30}\text{IrN}_2]^+$   $m/z$  527.2039 found  $m/z$  527.2019 and  $[\text{M} - \text{Cl} + \text{CH}_3\text{CN}]^+$  calculated for  $[\text{C}_{25}\text{H}_{35}\text{IrN}_3]^+$  570.2461 found 570.2440. NMR and MS data correspond to earlier reported values<sup>11</sup>

---

#### Chloride abstraction to obtain **Ir-p**

An  $\text{AgBF}_4$  stock solution (0.096 ml, 0.380 M, 0.037 mmol) in  $\text{CD}_3\text{CN}$  is added to a stirring solution of **S4** in  $\text{CD}_3\text{CN}$  (0.075 M, 0.489 ml, 0.037 mmol). The reaction immediately turns from an orange suspension to an orange/white cloudy mixture with increasing amounts of precipitate. The mixture is excluded from light and stirred for 20 min at room temperature. Thereafter, the mixture is filtered through a syringe filter (0.45  $\mu\text{m}$ ) and used without further purification (qt.).  $^1\text{H}$ -NMR (500 MHz,  $\text{CD}_3\text{CN}$ )  $\delta$  7.38 (d, 1H,  $J = 2.0$  Hz) 7.12 (s, 1H), 7.09 (d, 1H,  $J = 2.0$  Hz), 7.03 (s, 1H), 4.50 (m, 1H), 4.36 - 4.20 (m, 3H), 3.85 - 3.73 (m, 1H) 3.15 - 3.28 (m, 1H, 1H), 2.36 (s, 3H), 2.16 - 2.26 (m), 2.10 (s, 3H), 2.06 - 1.97 (m, 3H), 1.92 (s, 3H), 1.90 - 1.85 (m, 1H), 1.79 - 1.70 (m, 2H), 1.66 - 1.56 (m, 1H) 1.51 - 1.35 (m, 2H) 1.04 (t, 3H, 7.4 Hz).  $^{13}\text{C}$  NMR (126 MHz,  $\text{CD}_3\text{CN}$ )  $\delta$  174.12, 140.28, 136.63, 136.22, 135.82, 130.11, 129.68, 125.33, 122.63, 82.51, 82.31, 66.92, 64.94, 53.33, 34.51, 32.20, 30.54, 29.38, 24.81, 21.10, 18.64, 18.06, 11.45. ESI-(pos.)-MS-(TOF):  $[\text{M} - \text{BF}_4]^+$  calculated for  $[\text{C}_{23}\text{H}_{30}\text{IrN}_2]^+$   $m/z$  527.2039 found  $m/z$  527.2017

---

## NMR spectra of synthesized metal complexes

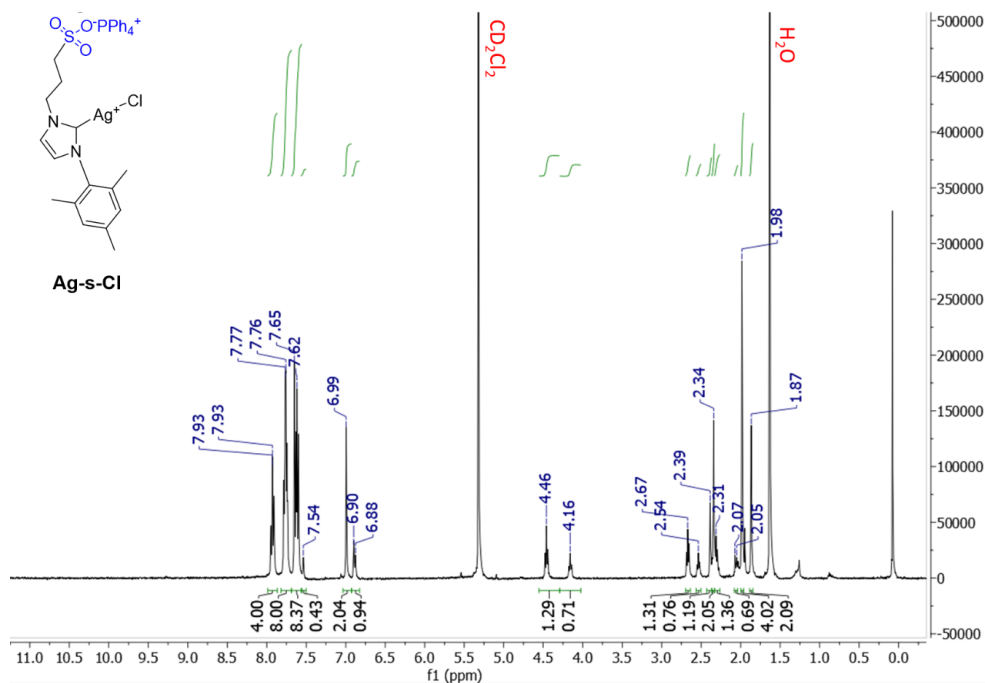


**Figure S1:**  $^1\text{H-NMR}$  spectrum of **Ag-s-Cl** in  $\text{CD}_2\text{Cl}_2$  (400 MHz)

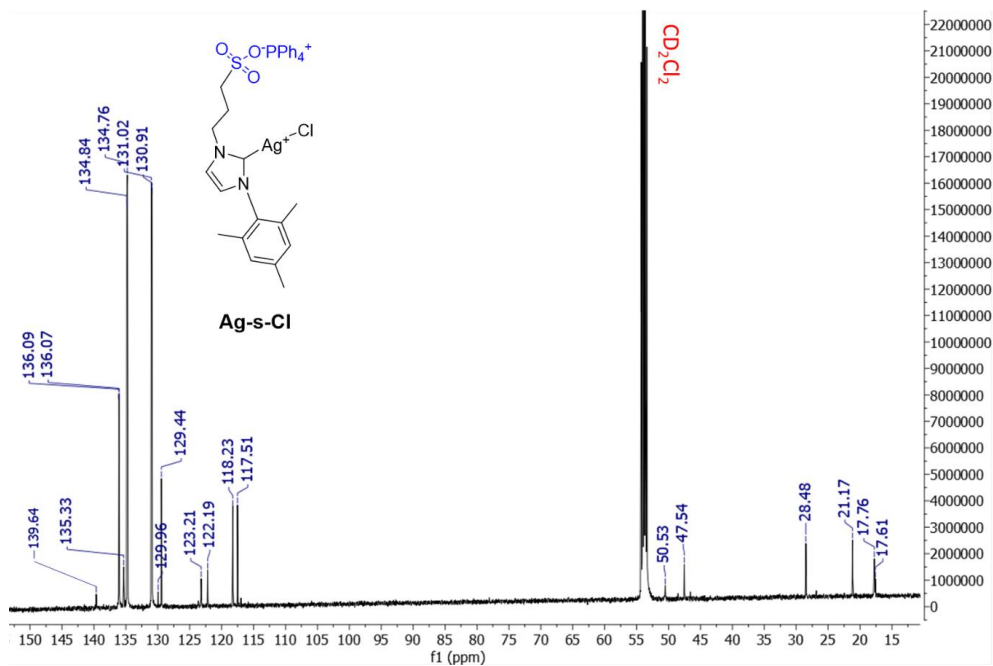


**Figure S2:**  $^{13}\text{C-NMR}$  spectrum of **Ag-s-Cl** in  $\text{CD}_2\text{Cl}_2$  (126 MHz)

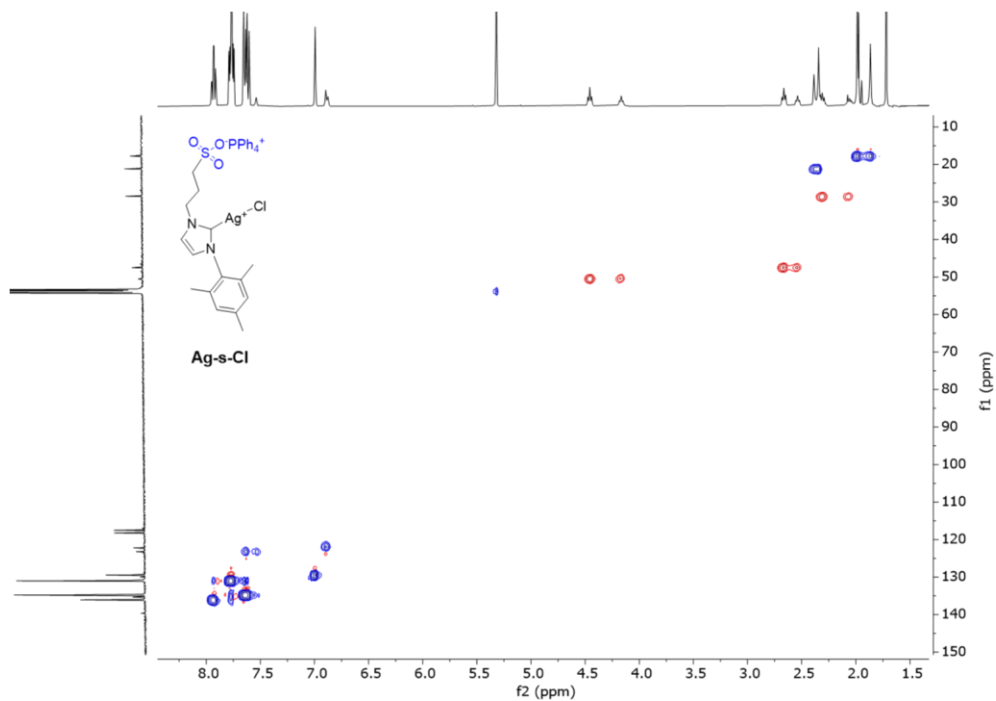


**Figure S3:**  $^1\text{H}$ - $^{13}\text{C}$ -HSQC-2D-NMR spectrum of **Ag-s-Cl**  $\text{CD}_2\text{Cl}_2$  (500 MHz)

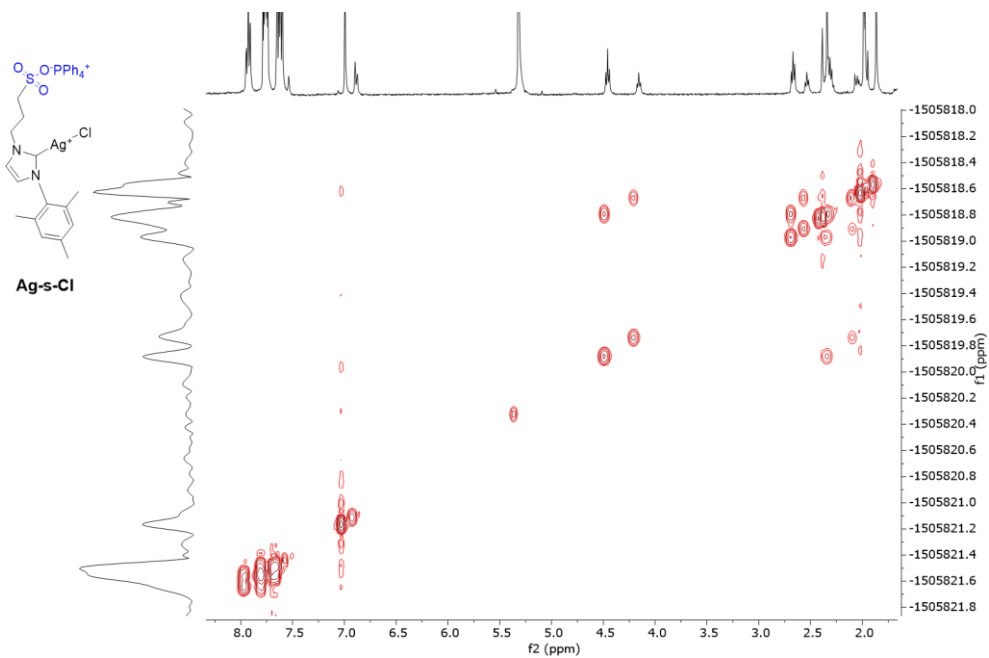


**Figure S4:**  $^1\text{H}$ -COSY-2D-NMR spectrum of **Ag-s-Cl**  $\text{CD}_2\text{Cl}_2$  (300 MHz)



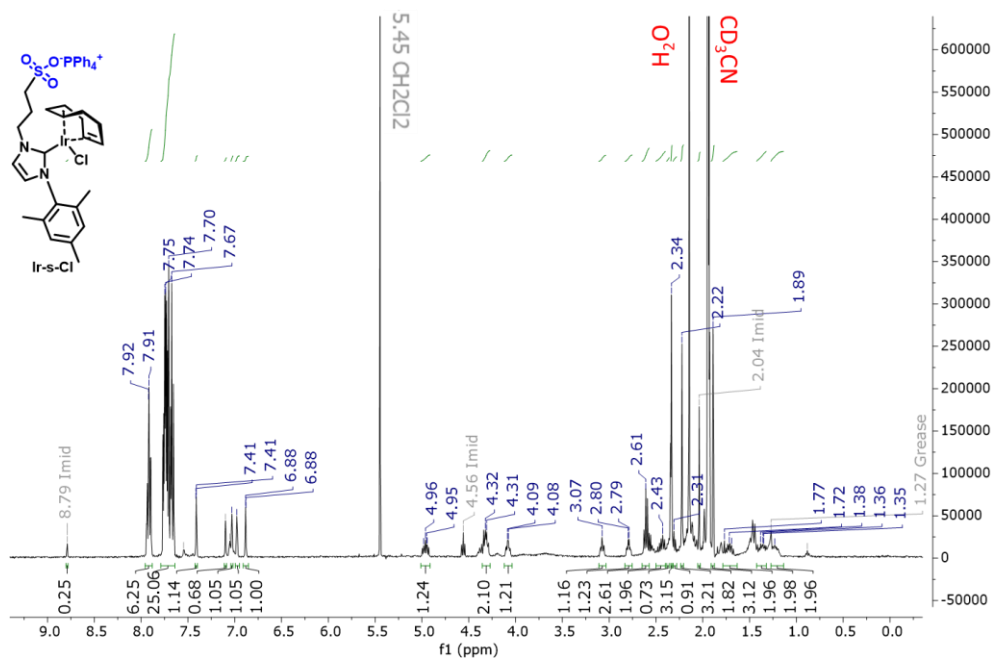


Figure S5:  $^1\text{H-NMR}$  spectrum of Ir-s-Cl in  $\text{CD}_3\text{CN}$  (400 MHz)

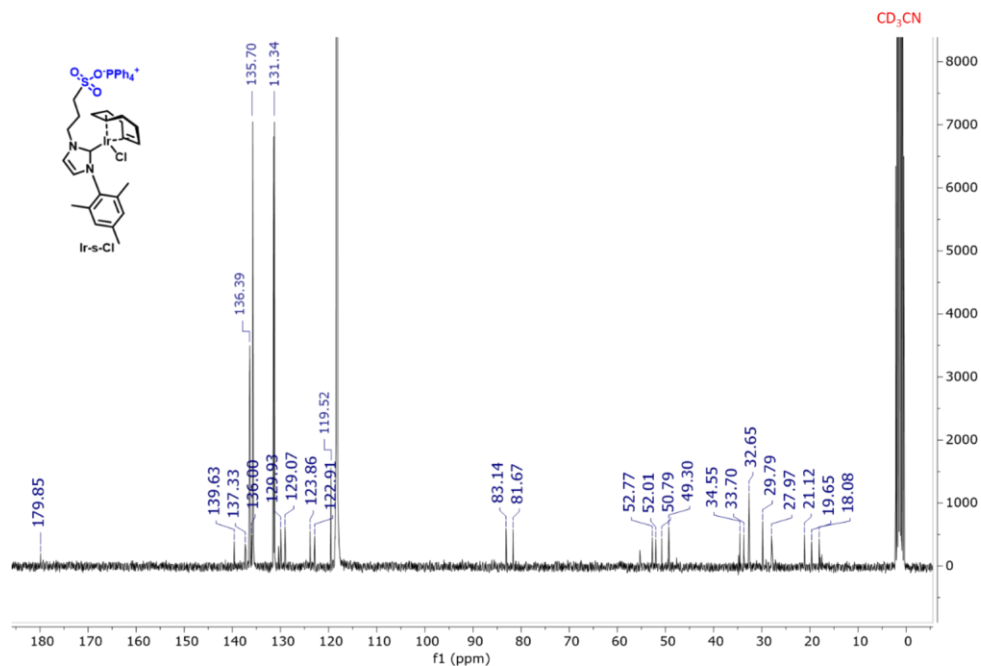


Figure S6:  $^{13}\text{C-NMR}$  spectrum of Ir-s-Cl in  $\text{CD}_3\text{CN}$  (75 MHz)

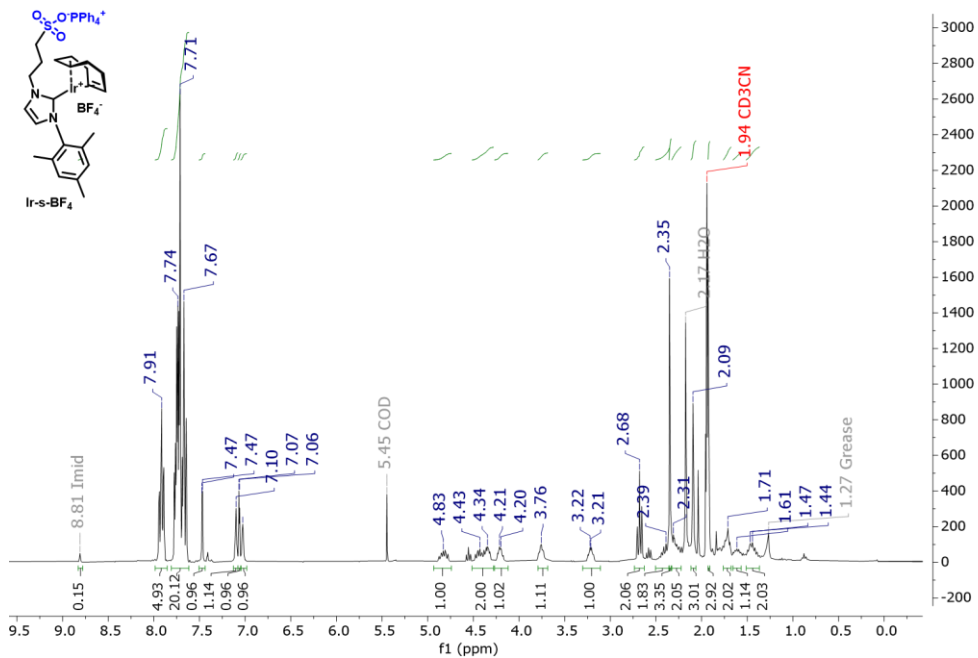


Figure S7: <sup>1</sup>H-NMR spectrum of Ir-s-BF<sub>4</sub> in CD<sub>3</sub>CN (300 MHz)

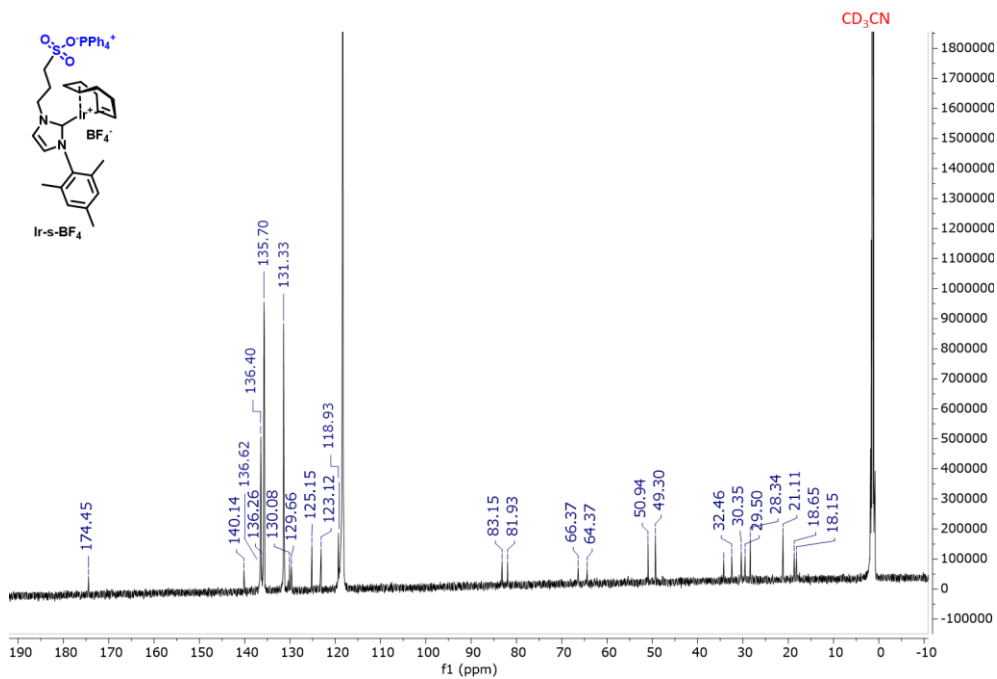
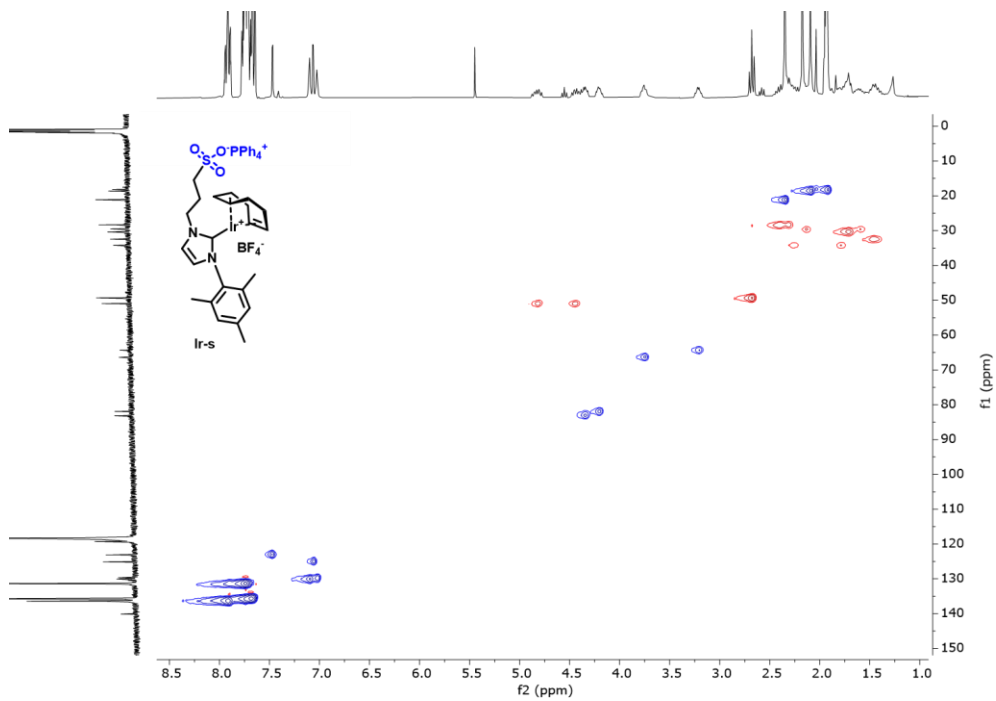
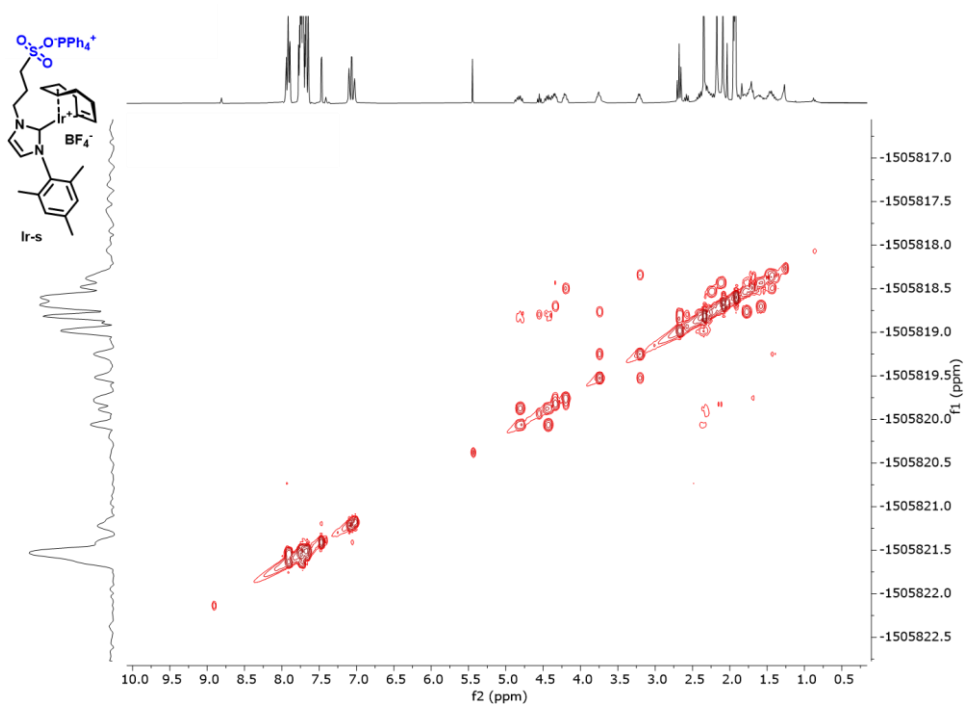


Figure S8: <sup>13</sup>C-NMR spectrum of Ir-s-BF<sub>4</sub> in CD<sub>3</sub>CN (126 MHz)



**Figure S9:**  $^1\text{H}$ - $^{13}\text{C}$ -HSQC-2D-NMR spectrum of **Ir-s**- $\text{BF}_4$   $\text{CD}_3\text{CN}$  (500 MHz)



**Figure S10:**  $^1\text{H}$ -COSY-2D-NMR spectrum of **Ag-s**- $\text{BF}_4$   $\text{CD}_3\text{CN}$  (500 MHz)

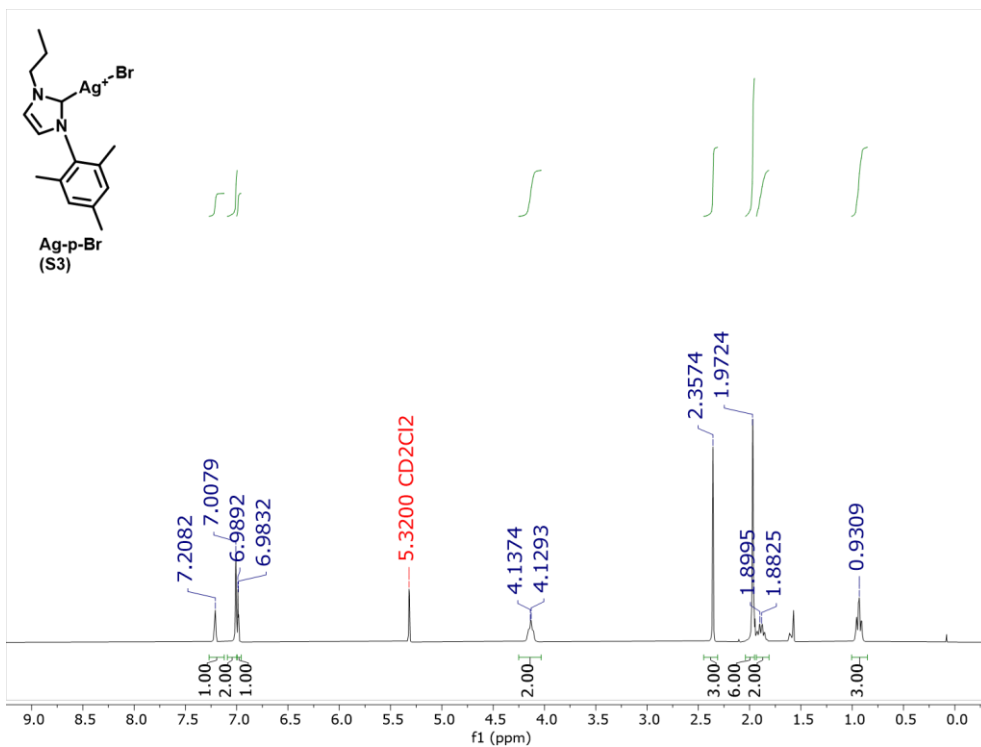


Figure S11: <sup>1</sup>H-NMR spectrum of **Ag-p-Br (S3)** in CD<sub>2</sub>Cl<sub>2</sub> (300 MHz)

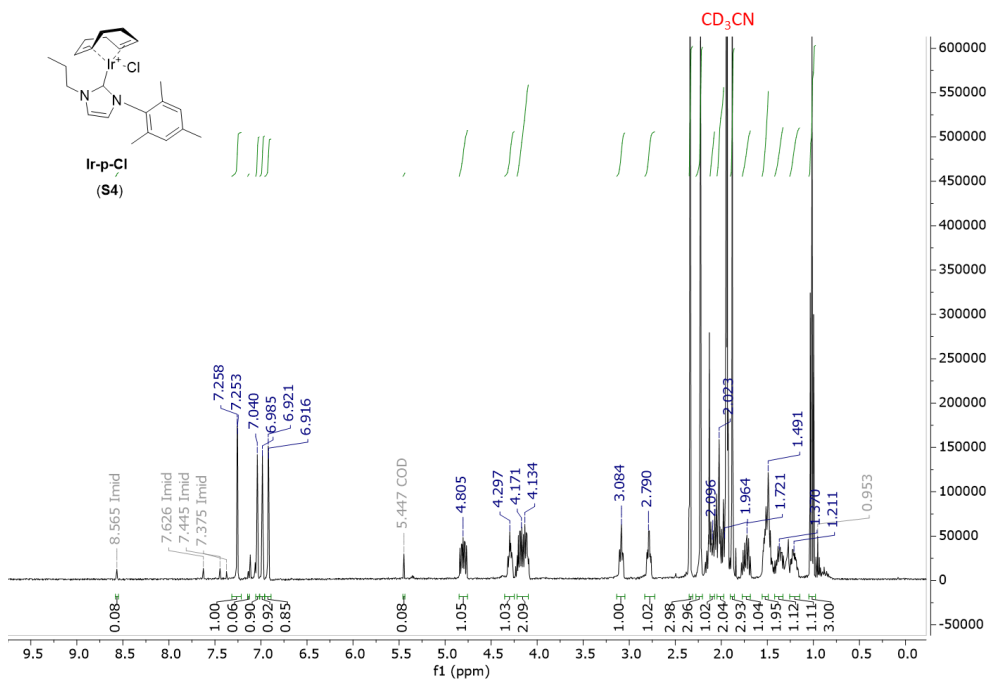
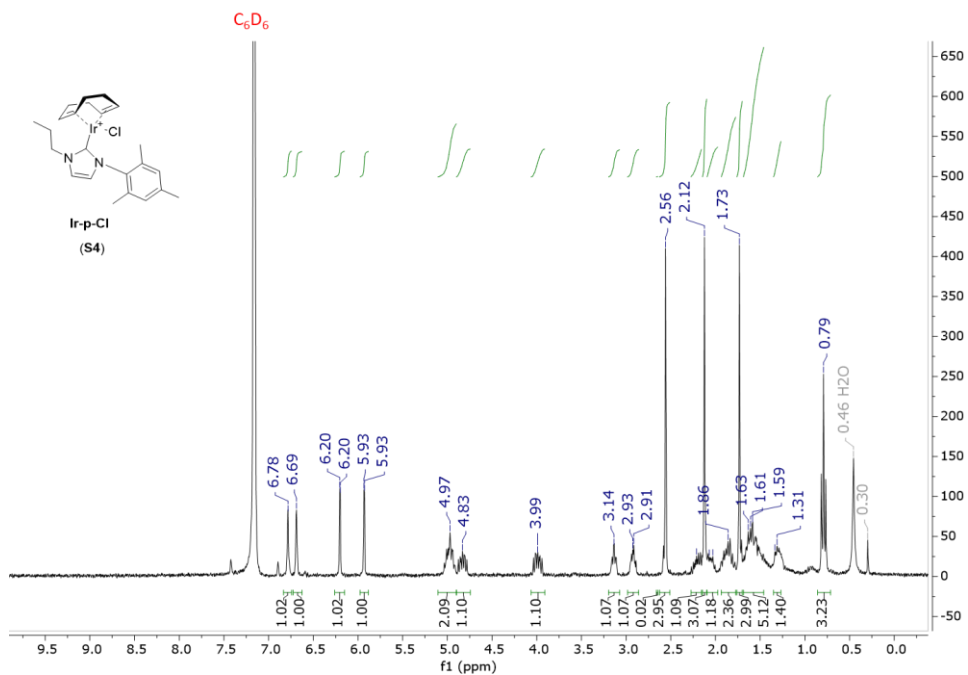
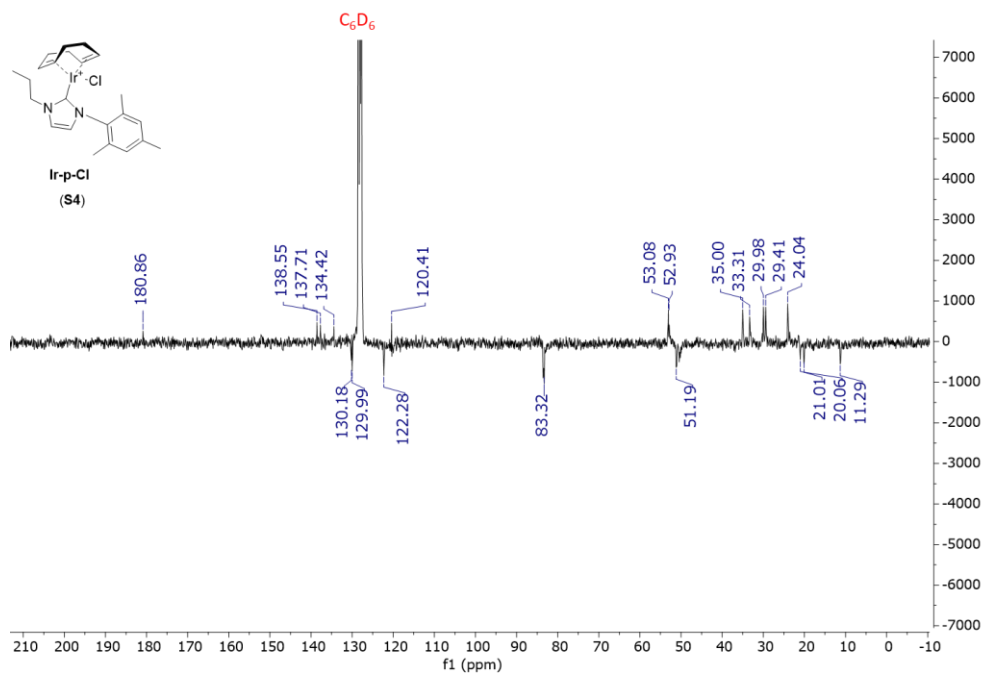


Figure S12: <sup>1</sup>H-NMR spectrum of **Ir-p-Cl (S4)** in CD<sub>3</sub>CN (400 MHz)



**Figure S13:** <sup>1</sup>H-NMR spectrum of Ir-p-Cl (S4) in C<sub>6</sub>D<sub>6</sub> (300 MHz)



**Figure S14:** <sup>13</sup>C-NMR spectrum of Ir-p-Cl (S4) in C<sub>6</sub>D<sub>6</sub> (300 MHz)

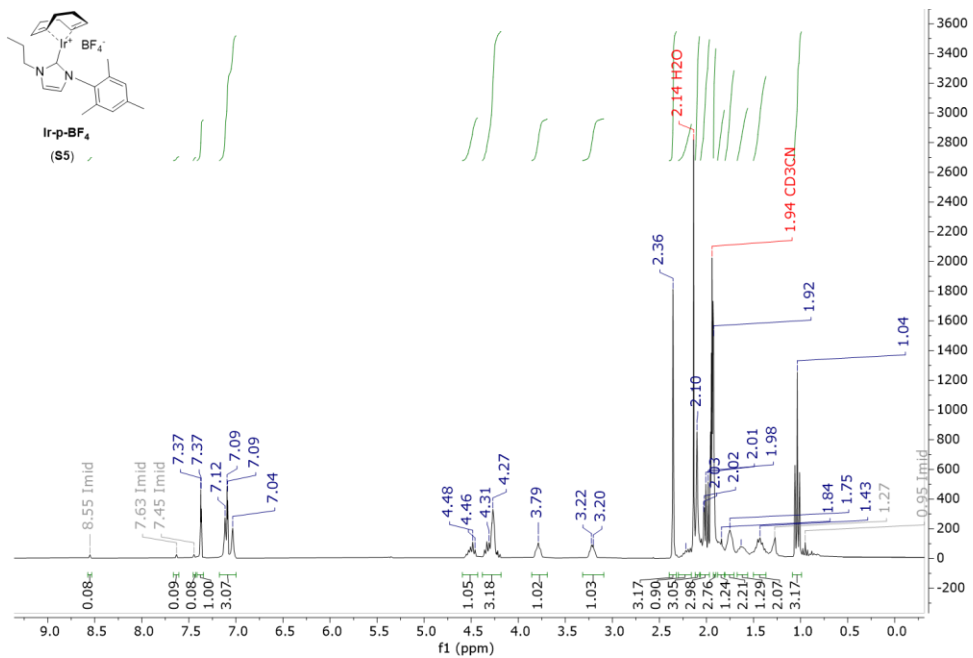


**Figure S15:** <sup>1</sup>H-NMR spectrum of Ir-p-BF<sub>4</sub> (S5) in CD<sub>3</sub>CN (300 MHz)

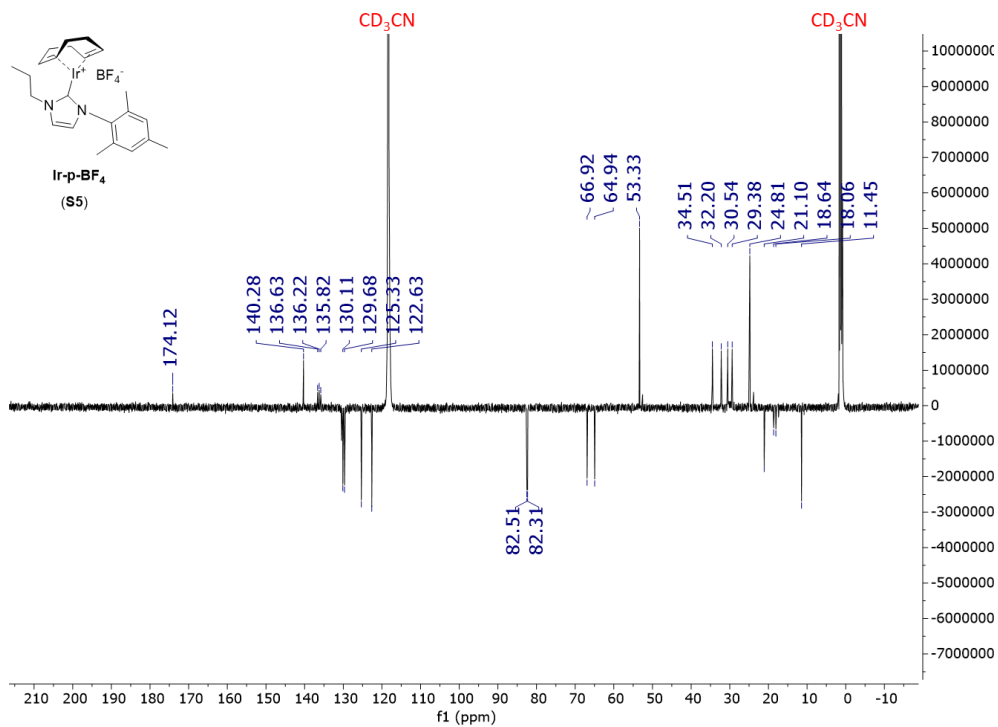
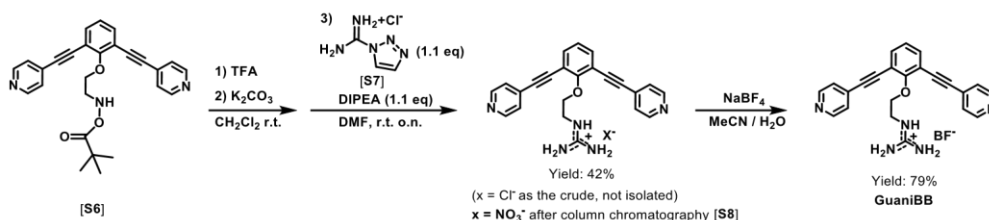


**Figure S16:** <sup>13</sup>C-NMR spectrum of Ir-p-BF<sub>4</sub> (S5) in CD<sub>3</sub>CN (126 MHz)

## Synthesis G-Sphere building block: **GuaniBB**



### Synthesis of **GuaniBB-NO<sub>3</sub>** (**13**)

**S8** was synthesized from **S6** in three consecutive steps as described below.

Note: step 1 and 2 are performed under atmospheric conditions

**Step 1)** 4 ml of TFA (52.3 mmol) was added to a solution of **S6** (0.480 g, 1.09 mmol) in 6 ml  $\text{CH}_2\text{Cl}_2$ . The mixture was stirred for one hour and the solvents were removed in vacuo and the resulting solids washed carefully with  $\text{CH}_2\text{Cl}_2$ .

**Step 2)** The resulting product of **step 1)** was taken up in a 1:1 mixture of  $\text{K}_2\text{CO}_3$  (sat. aq. 100 ml) and  $\text{CH}_2\text{Cl}_2$  (100 ml), the mixture is shaken vigorously and stirred for 5 min. Then, the mixture is then extracted, the aqueous layers is washed with  $\text{H}_2\text{O}$  (2x 20 ml) and all organic layers are collected. The crude product is concentrated (~2-5 ml) and transferred to a Schlenk. All solvents were removed under vacuum and the product (orange oil) was immediately used in the next step.

**Step 3)** 1*H*-pyrazole-1-carboxamide hydrochloride (**S7**) (0.178 g, 1.22 mmol, 1.1 eq) was added to the product in the Schlenk from **step 2)** and the system was flushed 3x Vac/Ar. Then, dry DMF (2.3 ml) and *N,N*-diisopropylethylamine (DIPEA, 0.22 ml, 1.22 mmol, 1.1 eq) were added sequentially. The resulting orange suspension was stirred at room temperature overnight. The solvents were removed in vacuo (60°C, 2 mbar) and the crude product was purified by column chromatography (Eluens 10%  $\text{KNO}_3$  (sat. Aq.) /  $\text{CH}_3\text{CN}$ ) to yield a light pink or beige solid (0.204 mg, 0.46 mmol, 42%)  $^1\text{H}$  NMR (400 MHz,  $\text{CD}_3\text{CN}$ )  $\delta$  8.63 (d,  $J = 6.0$  Hz, 4H), 7.65 (d,  $J = 7.7$  Hz, 2H), 7.47 (d,  $J = 6.0$  Hz, 4H), 7.26 (t,  $J = 7.7$  Hz, 2H), 6.45 (b, 4H), 4.45 (t,  $J = 4.9$  Hz, 2H), 3.64 (q,  $J = 5.3$  Hz, 2H).

### Ion exchange to furnish **GuaniBB**

**S8** (0.204 g, 0.46 mmol) and NaBF<sub>4</sub> (0.450 g, 4 mmol, 9 eq) were weighed in a round bottom flask, then a 1:1 mixture of H<sub>2</sub>O:CH<sub>3</sub>CN was added (6 ml total) and the beige solution was stirred for 15 min. Then, the solvents were removed in vacuo and water was added and the resulting suspension was filtered and washed twice with water. This procedure was repeated another time with the resulting product to ensure all ions were exchanged (again with 6 ml 1:1 H<sub>2</sub>O:CH<sub>3</sub>CN mixture and 0.450g of NaBF<sub>4</sub>). This furnished a white fluffy solid (0.170 g, 0.36 mmol, 79%) <sup>1</sup>H NMR (400 MHz, CD<sub>3</sub>CN) δ 8.64 (d, *J* = 5.7 Hz, 4H), 7.66 (d, *J* = 7.8 Hz, 2H), 7.47 (d, *J* = 5.7 Hz, 4H), 7.27 (t, *J* = 7.8 Hz, 1H), 6.57 (b, 1H), 6.06 (b, 4H), 4.45 (t, *J* = 4.9 Hz, 2H), 3.65 (q, *J* = 5.3 Hz, 2H). The spectra correspond to the those reported in literature<sup>12</sup>



## NMR spectra of **GuanibB** and **S8**

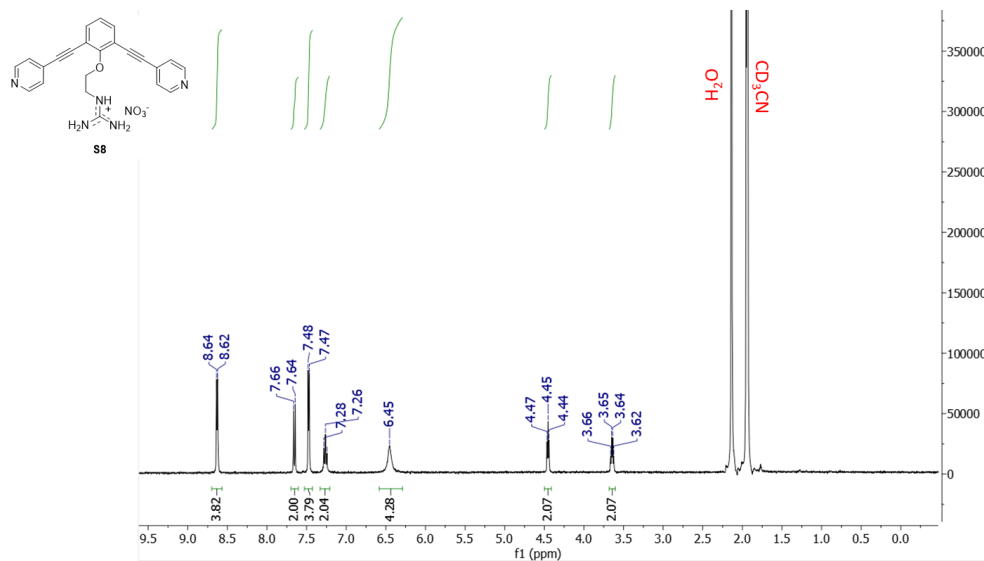


**Figure S17:** <sup>1</sup>H-NMR spectrum of **S8** in CD<sub>3</sub>CN (400 MHz)

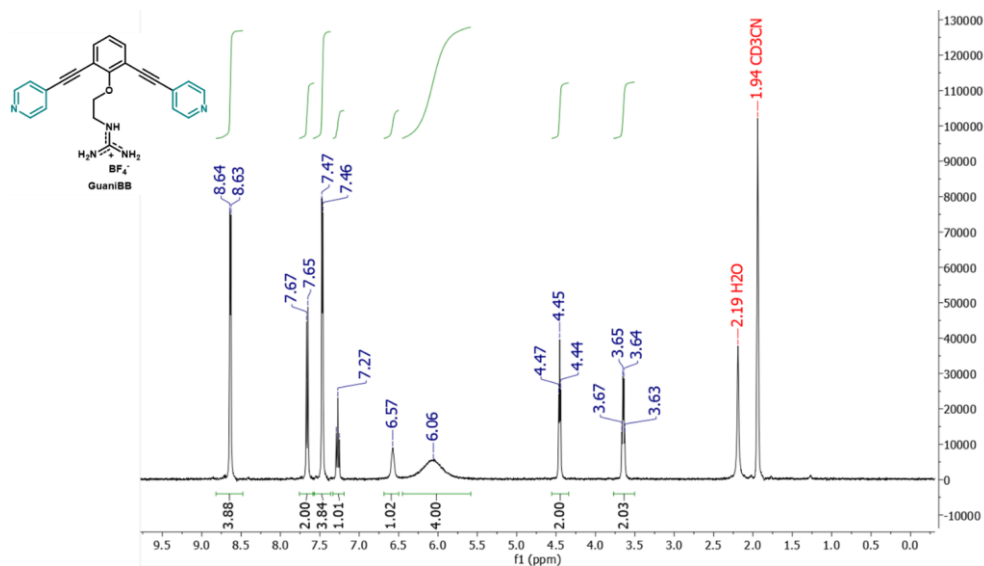


**Figure S18:** <sup>1</sup>H-NMR spectrum of **GuanibB** in CD<sub>3</sub>CN (300 MHz)

## Synthesis and characterization of **G-sphere** ( $M_{12}L_{24}$ )



### Pd-G-sphere synthesis ( $\text{Pd}_{12}\text{GuaniBB}_{24}$ )( $\text{BF}_4$ )<sub>48</sub>

This synthesis is based on a modified procedure developed in our group<sup>12</sup>

**GuaniBB** (4.7 mg, 10  $\mu\text{mol}$ ) was dissolved in  $\text{CD}_3\text{CN}$  (0.5 mL) in a vial equipped with a stirring bean and slightly heated to obtain a clear solution, then, a solution of  $\text{Pd}(\text{CH}_3\text{CN})_4(\text{BF}_4)_2$  (2.22 mg, 0.5  $\mu\text{mol}$ ) in  $\text{CD}_3\text{CN}$  (0.5 mL) was added to the mixture with a micropipette while stirring. The solution was carefully mixed back and forth to prevent any loss of material and ensure precise stoichiometry. The resulting solution was heated at 70 °C for 1h, leading to the quantitative formation of the sphere (**Pd-G-sphere**), which was confirmed by  $^1\text{H}$ -, DOSY-NMR and mass spectroscopy analysis.  $^1\text{H}$  NMR (300 MHz,  $\text{CD}_3\text{CN}$ )  $\delta$  8.90 (d,  $J = 6.6$  Hz, 4H), 7.80 – 7.61 (m, 6H), 7.27 (t,  $J = 7.7$  Hz, 1H), 6.70 (t,  $J = 5.6$  Hz, 1H), 6.24 (b, 4H), 4.40 (t,  $J = 4.5$  Hz, 2H), 3.69 (q,  $J = 5.6, 4.5$  Hz, 2H). MS (ESI):  $m/z$  (calc. for  $[\text{M} - 14(\text{BF}_4^-)]_{14+}$  957.6354, found 957.6409 (calc. for  $[\text{M} - 13(\text{BF}_4^-)]_{13+}$  1037.9250, found 1037.9218 (calc. for  $[\text{M} - 12(\text{BF}_4^-)]_{12+}$  1131.6671, found 1131.6667 (calc. for  $[\text{M} - 11(\text{BF}_4^-)]_{11+}$  1242.4546, found 1242.4538 (calc. for  $[\text{M} - 10(\text{BF}_4^-)]_{10+}$  1375.4003, found 1375.3997 (calc. for  $[\text{M} - 9(\text{BF}_4^-)]_{9+}$  1537.8898, found 1537.8884 (calc. for  $[\text{M} - 8(\text{BF}_4^-)]_{8+}$  1740.8768 found 1740.8737, (calc. for  $[\text{M} - 7(\text{BF}_4^-)]_{7+}$  2002.0025 found 2001.9993 (calc. for  $[\text{M} - 6(\text{BF}_4^-)]_{6+}$  2350.1702 found 2350.1647. DOSY NMR ( $\text{CD}_3\text{CN}$ , 298 K):  $\log D = -9.58$

### Pt-G-sphere synthesis ( $\text{Pt}_{12}\text{GuaniBB}_{24}$ )( $\text{BF}_4$ )<sub>48</sub>

This synthesis is based on a literature procedure developed in our group<sup>4,13</sup>

To a pressure resistant microwave vial, 4  $\mu\text{L}$  of a stock solution containing  $\text{PPh}_4\text{Cl}$  (94.5 mM, 0.385  $\mu\text{mol}$ ) was added. The vial was equipped with a septum and the solvent was removed under vacuum (>30 min). Then, **GuaniBB** (**1**) (4.7 mg, 10  $\mu\text{mol}$ , 1 eq.) and  $\text{Pt}(\text{CH}_3\text{CN})_4(\text{BF}_4)_2$  (3 mg, 5.63  $\mu\text{mol}$ , 0.56 eq.) were weighted and added to the vial. The vial was again

equipped with a septum and flushed with argon/vacuum 3 times (through a needle in the septum). Then, 1 mL dry degassed CD<sub>3</sub>CN was added to the vial. Thereafter, the septum was replaced with an aluminium cap under Ar flow and firmly closed. The pale yellow solution was first stirred at room temperature for 20 min and was then placed in a preheated oil bath to be stirred for 48 hours at 130 °C. The resulting solution was filtered through a syringe filter (0.45 μm) and characterized with <sup>1</sup>H-NMR, MS and DOSY. <sup>1</sup>H NMR (300 MHz, CD<sub>3</sub>CN) δ 8.90 (m, 4H) 7.65 (m, 6H), 7.27 (m, 1H), 6.70 (b, 1H), 6.24 (b, 4H), 4.42 (b, 2H), 3.69 (b, 2H). MS (ESI): m/z (calc. for [M – 14(BF<sub>4</sub><sup>-</sup>)]14+, 1033.6215 found 1033.6262 (calc. for [M – 13(BF<sub>4</sub><sup>-</sup>)]13+, 1119.8236 found 1119.8296 (calc. for [M – 12(BF<sub>4</sub><sup>-</sup>)]12+, 1220.3922 found 1220.4313 (calc. for [M – 11(BF<sub>4</sub><sup>-</sup>)]11+ 1339.1558, found 1339.1626 (calc. for [M – 10(BF<sub>4</sub><sup>-</sup>)]10+ 1481.7722, found 1481.7770 (calc. for [M – 9(BF<sub>4</sub><sup>-</sup>)]9+ 1656.0803, found 1656.0844 (calc. for [M – 8(BF<sub>4</sub><sup>-</sup>)]8+) 1873.9653 found 1873.9696, (calc. for [M – 7(BF<sub>4</sub><sup>-</sup>)]7+) 2153.9619 found 2153.9667 (calc. for [M – 6(BF<sub>4</sub><sup>-</sup>)]6+) 2527.4560 found 2527.4636. DOSY-NMR (CD<sub>3</sub>CN, 298 K): log D = –9.58

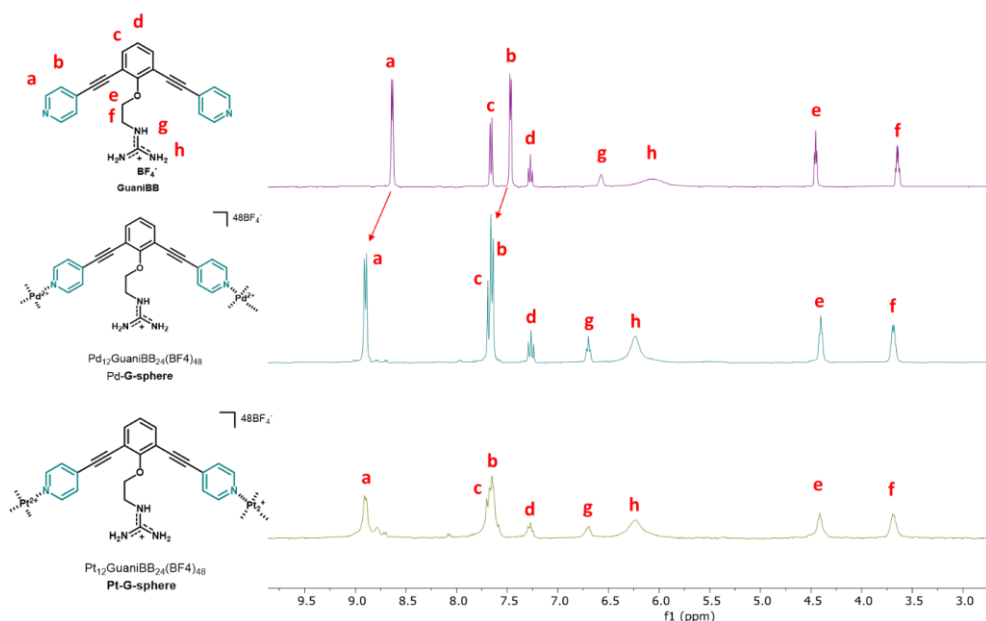


**Figure S19:** <sup>1</sup>H-NMR (298 K, CD<sub>3</sub>CN) of **GuaniBB** (top), **Pd-G-sphere** (Pd<sub>12</sub>GuaniBB<sub>24</sub>(BF<sub>4</sub>)<sub>48</sub>) (middle) and **Pt-G-sphere** (Pt<sub>12</sub>GuaniBB<sub>24</sub>(BF<sub>4</sub>)<sub>48</sub>) (bottom).

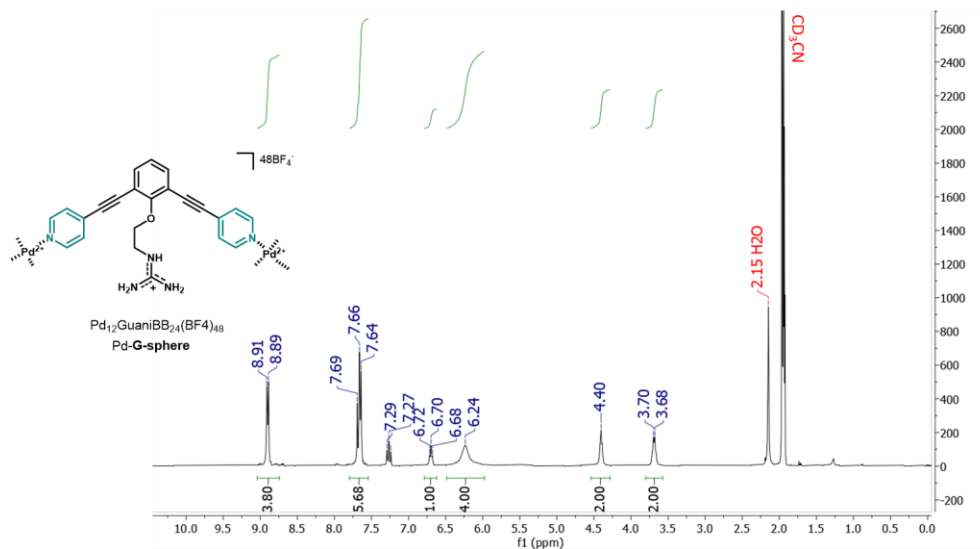


**Figure S20:** <sup>1</sup>H-NMR spectrum of Pd-G-sphere (Pd<sub>12</sub>GuaniBB<sub>24</sub>(BF<sub>4</sub>)<sub>48</sub>) in CD<sub>3</sub>CN (300 MHz)

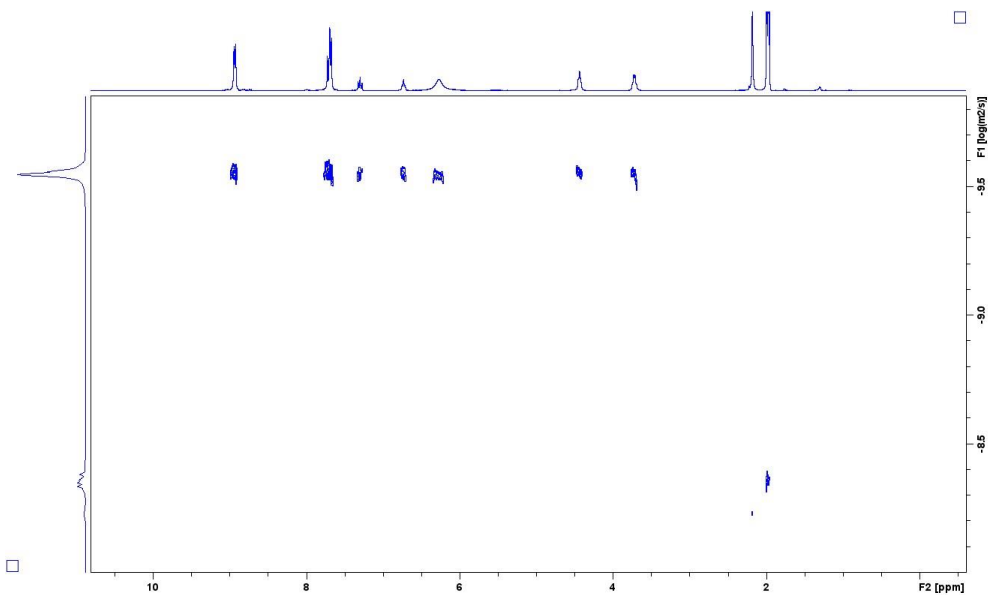


**Figure S21:** <sup>1</sup>H-DOSY-NMR spectrum of Pd-G-sphere (Pd<sub>12</sub>GuaniBB<sub>24</sub>(BF<sub>4</sub>)<sub>48</sub>) in CD<sub>3</sub>CN at 25 °C (300 MHz)

## NMR and MS spectra of **Pt-G-sphere** and **Pd-G-sphere**

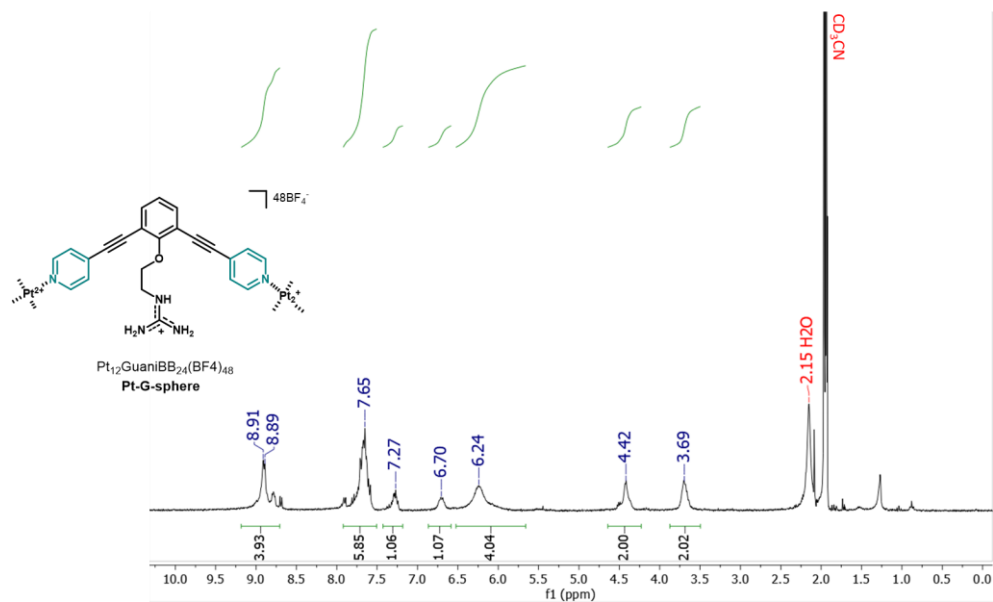


**Figure S22:** <sup>1</sup>H-NMR spectrum of **Pt-G-sphere** (Pt<sub>12</sub>GuaniBB<sub>24</sub>(BF<sub>4</sub>)<sub>48</sub>) in CD<sub>3</sub>CN (300 MHz)

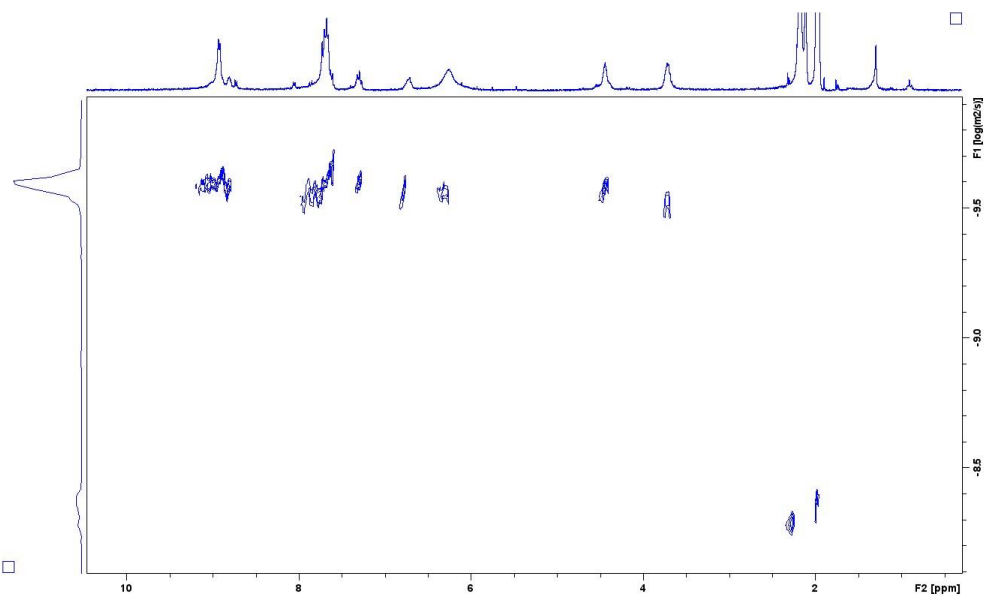


**Figure S23:** <sup>1</sup>H-DOSY-NMR spectrum of **Pt-G-sphere** (Pt<sub>12</sub>GuaniBB<sub>24</sub>(BF<sub>4</sub>)<sub>48</sub>) in CD<sub>3</sub>CN at 25 °C (300 MHz)

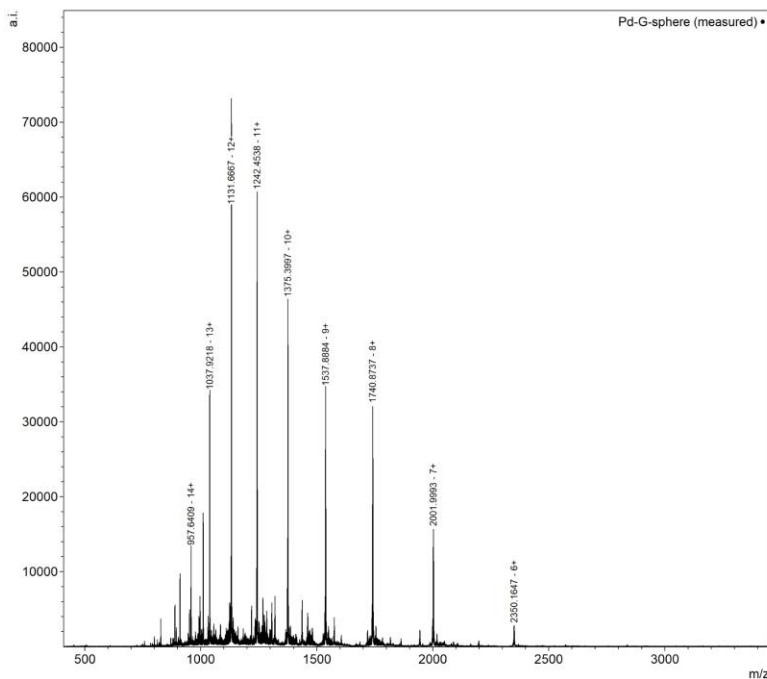


**Figure S24:** CSI-TOF mass spectrum (full spectrum) of the **Pd-G-sphere** ( $\text{Pd}_{12}\text{GuaBB}_{24}$ )( $\text{BF}_4$ ) $_{48}$ , with a spray temperature of  $-40^\circ\text{C}$  and a dry gas temperature of  $-35^\circ\text{C}$ .

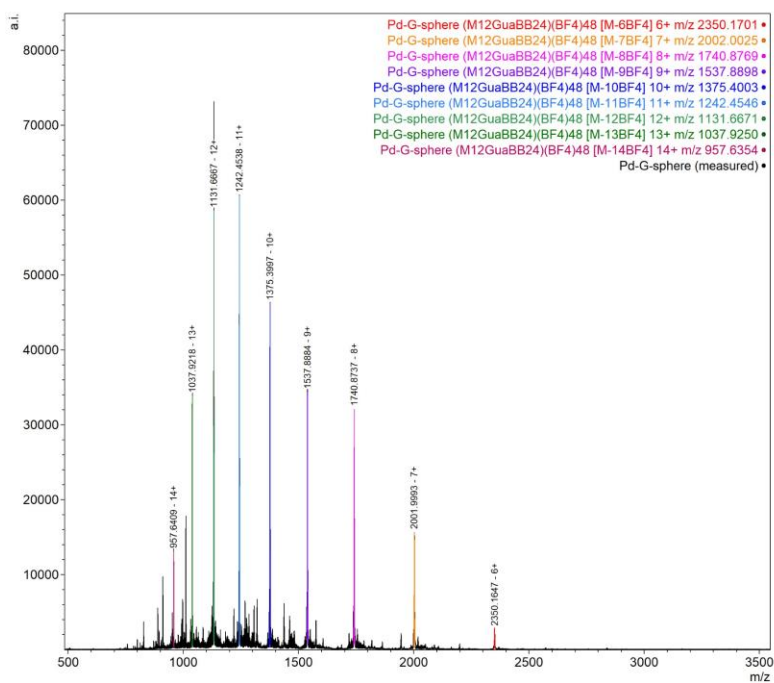


**Figure S25:** CSI-TOF mass spectrum (full spectrum) of the **Pd-G-sphere** ( $\text{Pd}_{12}\text{GuaBB}_{24}$ )( $\text{BF}_4$ ) $_{48}$ , with a spray temperature of  $-40^\circ\text{C}$  and a dry gas temperature of  $-35^\circ\text{C}$ , overlaid with simulated isotopic patterns in colour.

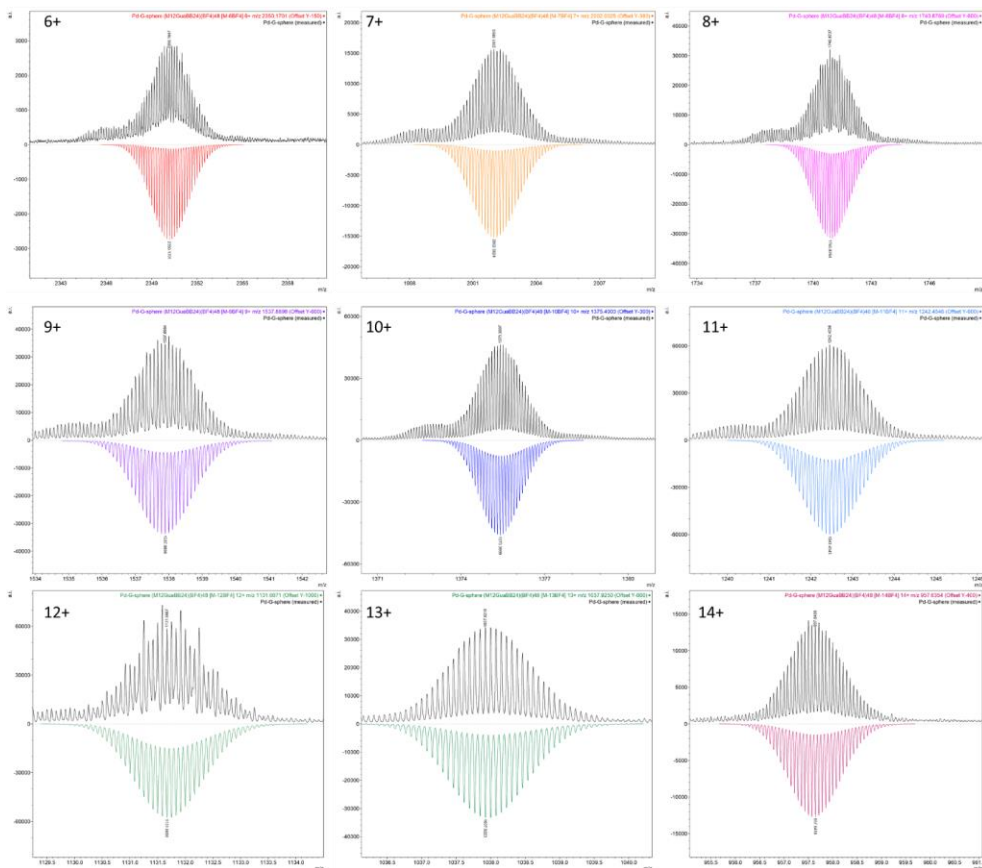


**Figure S26:** CSI-TOF mass spectrum, zoomed spectra of differently charged species of the **Pd-G-sphere** ( $\text{Pd}_{12}\text{GuaniBB}_{24}$ )( $\text{BF}_4$ ) $_{48}$ , compared with the simulated isotopic patterns in colour. With a spray temperature of  $-40\text{ }^\circ\text{C}$  and a dry gas temperature of  $-35\text{ }^\circ\text{C}$ , overlaid with simulated isotopic patterns in colour.

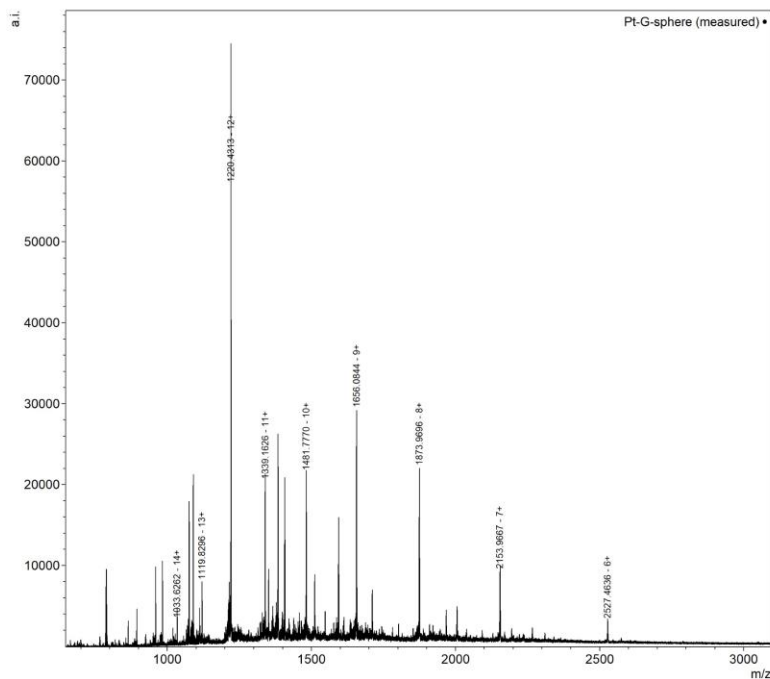


**Figure S27:** CSI-TOF mass spectrum (full spectrum) of the **Pt-G-sphere** ( $\text{Pt}_{12}\text{GuaniBB}_{24}$ )( $\text{BF}_4$ )<sub>48</sub>, with a spray temperature of  $-40\text{ }^\circ\text{C}$  and a dry gas temperature of  $-35\text{ }^\circ\text{C}$

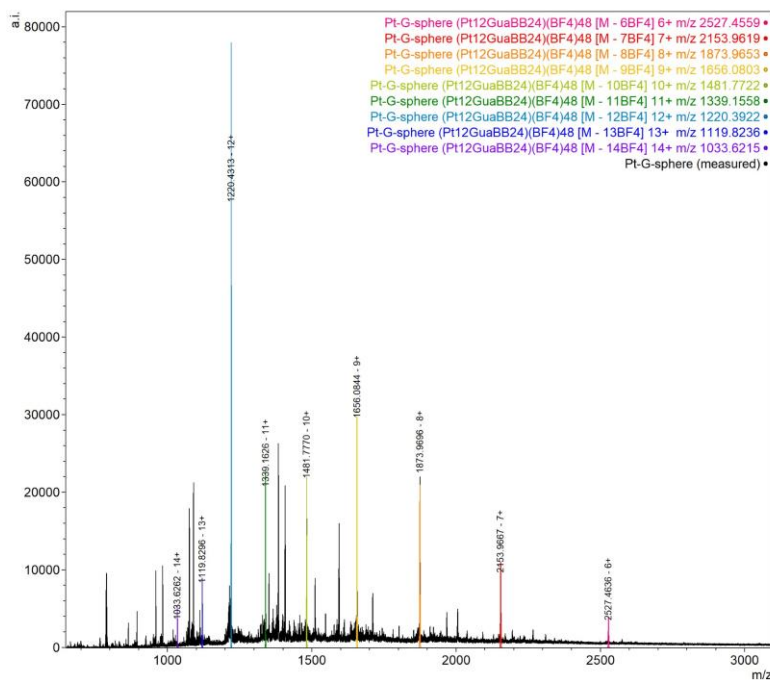


**Figure S28:** CSI-TOF mass spectrum (full spectrum) of the **Pt-G-sphere** ( $\text{Pt}_{12}\text{GuaniBB}_{24}$ )( $\text{BF}_4$ )<sub>48</sub>, with a spray temperature of  $-40\text{ }^\circ\text{C}$  and a dry gas temperature of  $-35\text{ }^\circ\text{C}$ , overlaid with simulated isotopic patterns in colour.



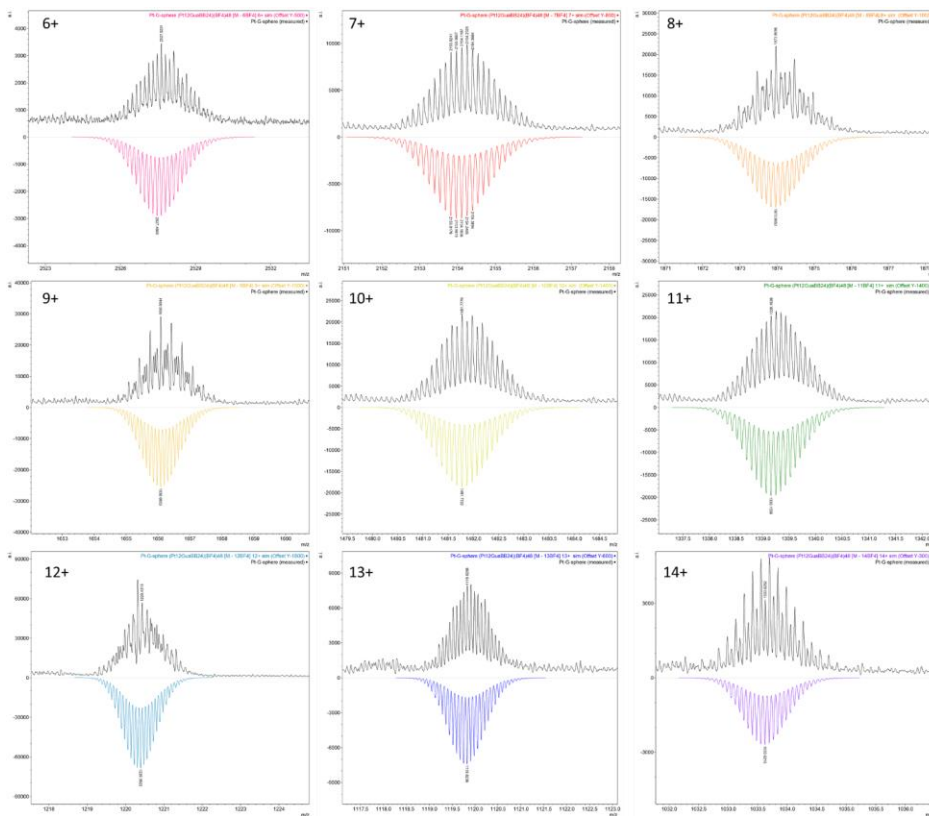


**Figure S29:** CSI-TOF mass spectrum, zoomed spectra of differently charged species of the **Pt-G-sphere** ( $\text{Pt}_{12}\text{GuaniBB}_{24}(\text{BF}_4)_{48}$ ), compared with the simulated isotopic patterns in colour. With a spray temperature of  $-40\text{ }^\circ\text{C}$  and a dry gas temperature of  $-35\text{ }^\circ\text{C}$ , overlaid with simulated isotopic patterns in colour.

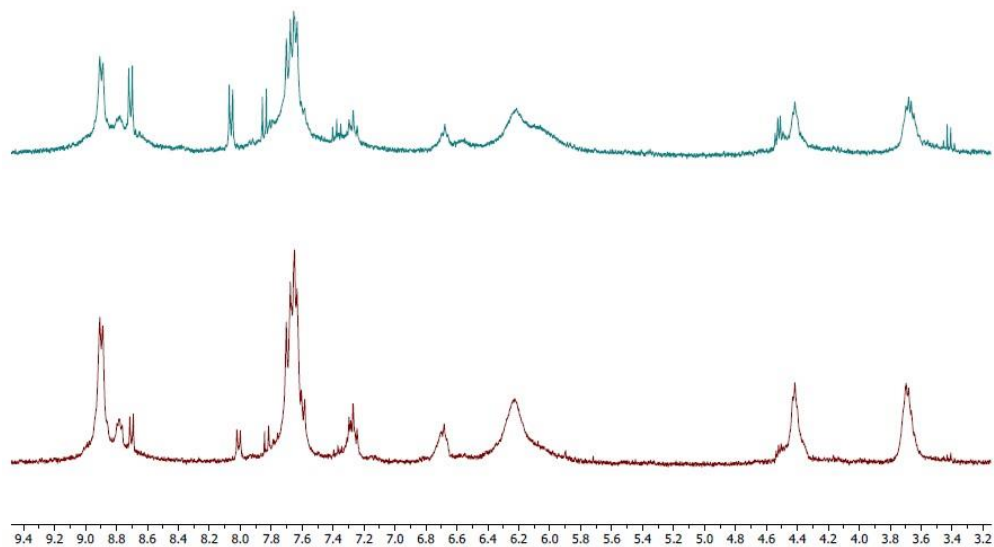


**Figure S30:**  $^1\text{H-NMR}$  (298K,  $\text{CD}_3\text{CN}$ ) of **Pt-G-Sphere** ( $\text{Pt}_{12}\text{GuaniBB}_{24}(\text{BF}_4)_{48}$ ) prepared with 6.0 eq. Pt-precursor (top), and **Pt-G-Sphere** ( $\text{Pt}_{12}\text{GuaniBB}_{24}(\text{BF}_4)_{48}$ ) prepared with 0.56 eq. Pt-precursor (bottom).

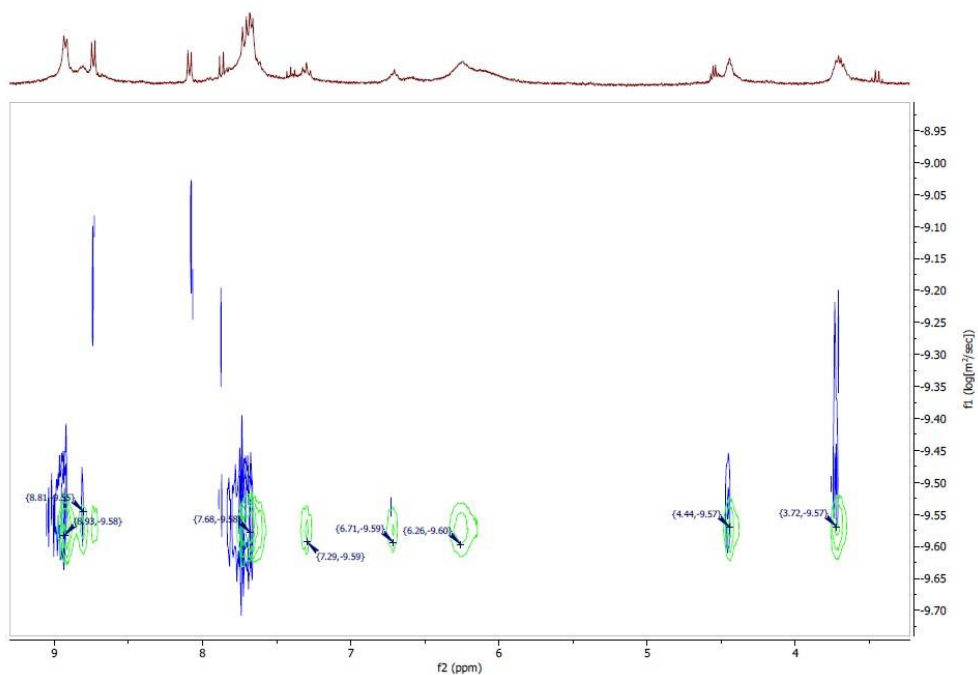


**Figure S31:**  $^1\text{H}$ -DOSY-NMR spectra of **Pt-G-Sphere** ( $\text{Pt}_{12}\text{GuaniBB}_{24}(\text{BF}_4)_{48}$ ) prepared with 6.0 eq. Pt-precursor at 500 MHz (blue), and **Pt-G-Sphere** ( $\text{Pt}_{12}\text{GuaniBB}_{24}(\text{BF}_4)_{48}$ ) prepared with 0.56 eq. Pt-precursor at 300 MHz (green), both in  $\text{CD}_3\text{CN}$  at  $25^\circ\text{C}$ .

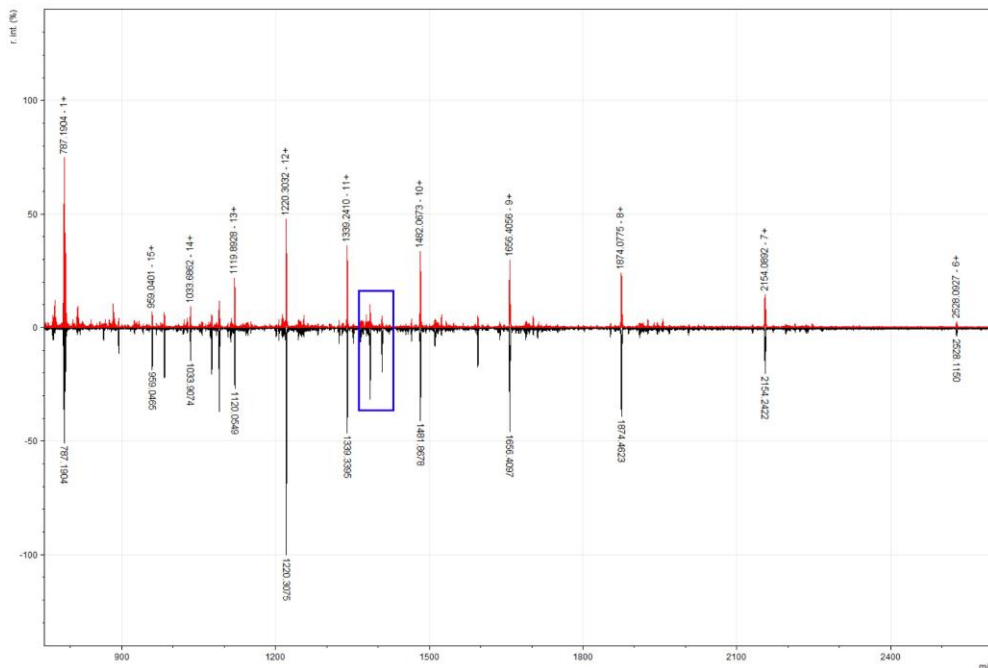


**Figure S32:** CSI-TOF mass spectrum of **Pt-G-Sphere** ( $\text{Pt}_{12}\text{GuaniBB}_{24}(\text{BF}_4)_{48}$ ) prepared with 6.0 eq. Pt-precursor (top, red), and **Pt-G-Sphere** ( $\text{Pt}_{12}\text{GuaniBB}_{24}(\text{BF}_4)_{48}$ ) prepared with 0.56 eq. Pt-precursor (bottom, black). Blue box indicates the  $\text{M}_9\text{L}_{18}$  (left peak) and  $\text{M}_8\text{L}_{16}$  (right peak) species, which are relatively less present in the top spectrum with 6.0 eq. Pt-precursor.

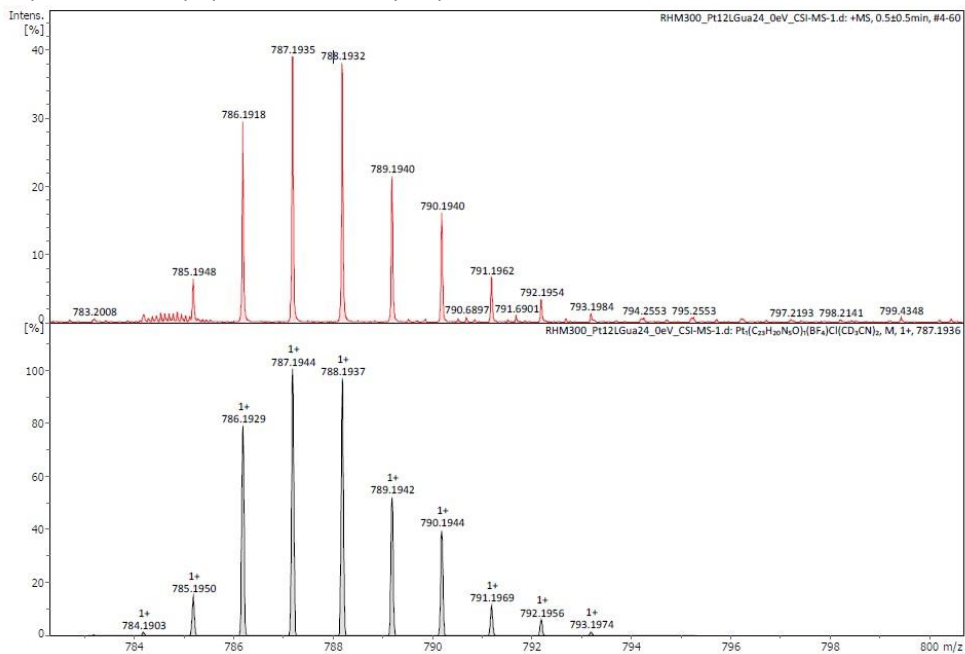


**Figure S33:** Zoom in of the increased peak at 787.1935 Da (top) and simulated spectrum of PtGuaniBB(CD<sub>3</sub>CN)<sub>2</sub>ClBF<sub>4</sub><sup>+</sup> (bottom). **(ESI-(pos.)-MS-(TOF):** [M – BF<sub>4</sub>]<sup>+</sup> calculated for [PtC<sub>27</sub>H<sub>20</sub>D<sub>6</sub>N<sub>7</sub>OBF<sub>4</sub>Cl]<sup>+</sup> m/z 787.1944 found m/z 787.1935)

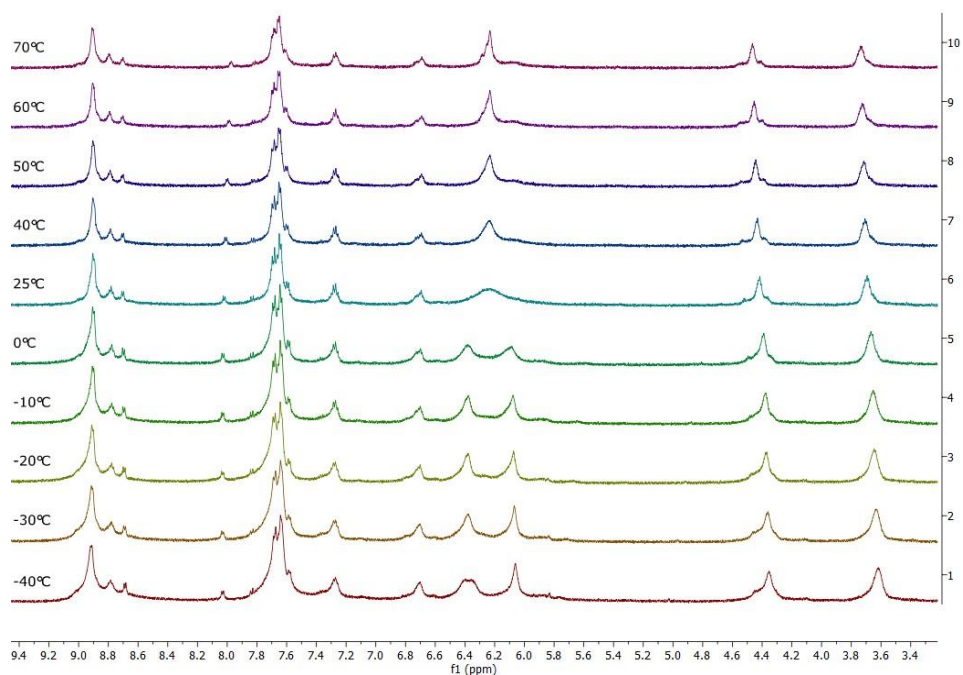


**Figure S34:** <sup>1</sup>H-NMR spectra of **Pt-G-Sphere** (Pt<sub>12</sub>GuaniBB<sub>24</sub>(BF<sub>4</sub>)<sub>48</sub>) in CD<sub>3</sub>CN (500MHz) at different temperatures

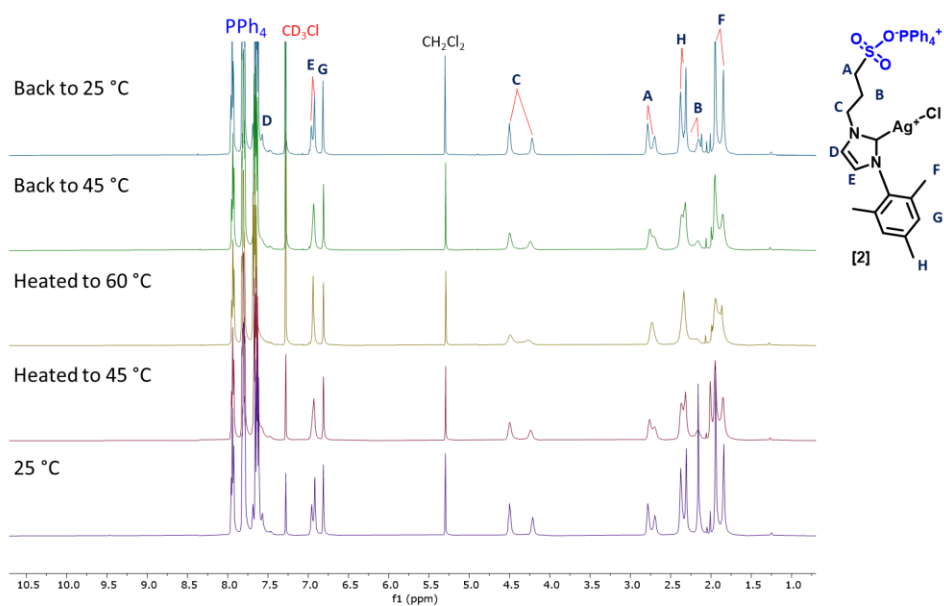
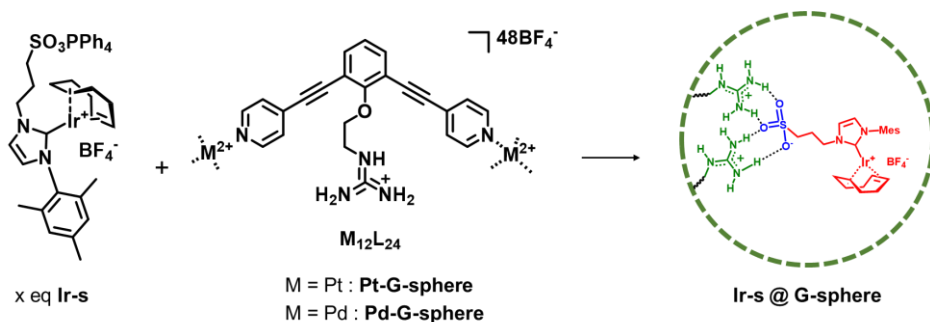


**Figure S35:** Temperature resolved <sup>1</sup>H-NMR spectra of **Ag-s-Cl** in CDCl<sub>3</sub> (500MHz)

## Binding experiments ( $^1\text{H}$ -NMR studies)



The binding behavior G-sphere towards Ir-s was studied by  $^1\text{H}$ -NMR titration and  $^1\text{H}$ -DOSY NMR experiments. All experiments were carried out at room temperature in  $\text{CD}_3\text{CN}$ . For the DOSY experiments, to 0.5 ml solutions of the sphere (0.42 mM **G-sphere/M-sphere** either Pd or Pt sphere) was added either 27, 40 or 80  $\mu\text{L}$  metal precursor (Ir-s 62.6 mM) corresponding to 8, 12 and 24 equivalents respectively. The corresponding spectra can be found in the following pages (Figure S36-39). Additionally, the control groups (**Ir-p + Pt-G-sphere** and **Ir-s + M-sphere**) were evaluated on their binding behavior with  $^1\text{H}$ -DOSY-NMR and, as expected, the lack of encapsulation is evident from the substantially different diffusion constants of the host and guest upon mixing (Figure S40 and Figure S41 for **Ir-p + Pt-G-sphere** and **Ir-s + Msphere** respectively).

### $^1\text{H}$ -NMR DOSY spectra of Ir-s @ Pd-G-sphere

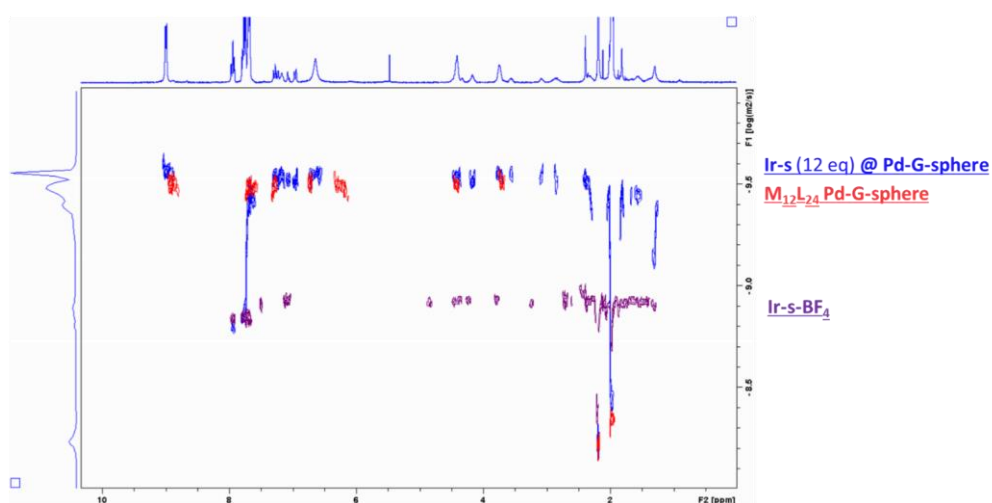


**Figure S36:**  $^1\text{H}$ -DOSY-NMR spectrum of **Ir-s (12 eq) @ Pd-G-sphere** (blue) and reference spectra of **Ir-s- $\text{BF}_4$**  (purple) and **Pd-G-sphere** (red), all in  $\text{CD}_3\text{CN}$  at  $25^\circ\text{C}$  (300 MHz)

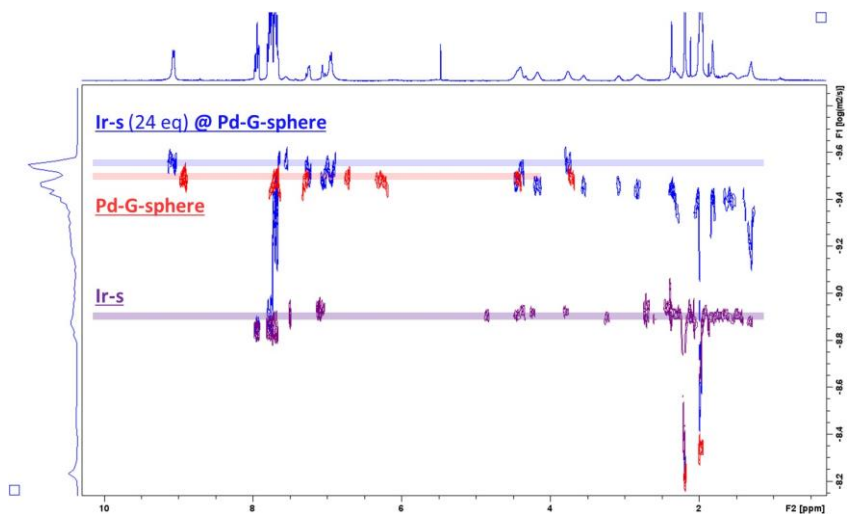


**Figure S37:**  $^1\text{H}$ -DOSY-NMR spectrum of **Ir-s (24 eq) @ Pd-G-sphere** (blue) and reference spectra of **Ir-s** (purple) and **Pd-G-sphere** (red), all in  $\text{CD}_3\text{CN}$  at  $25^\circ\text{C}$  (300 MHz)

### $^1\text{H}$ -NMR DOSY spectra of **Ir-s @ Pt-G-sphere**

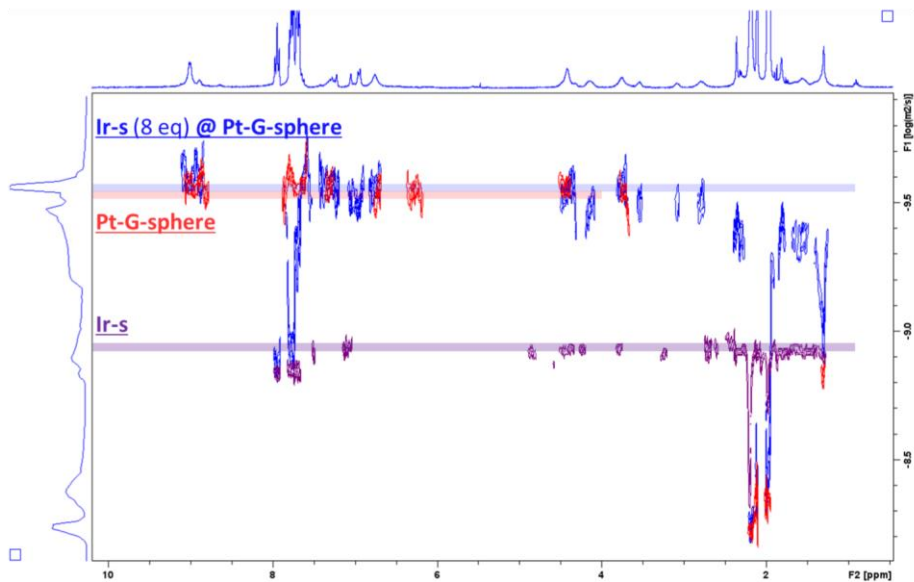


**Figure S38:**  $^1\text{H}$ -DOSY-NMR spectrum of **Ir-s (8 eq) @ Pt-G-sphere** (blue) and reference spectra of **Ir-s** (purple) and **Pt-G-sphere** (red), all in  $\text{CD}_3\text{CN}$  at  $25^\circ\text{C}$  (300 MHz)

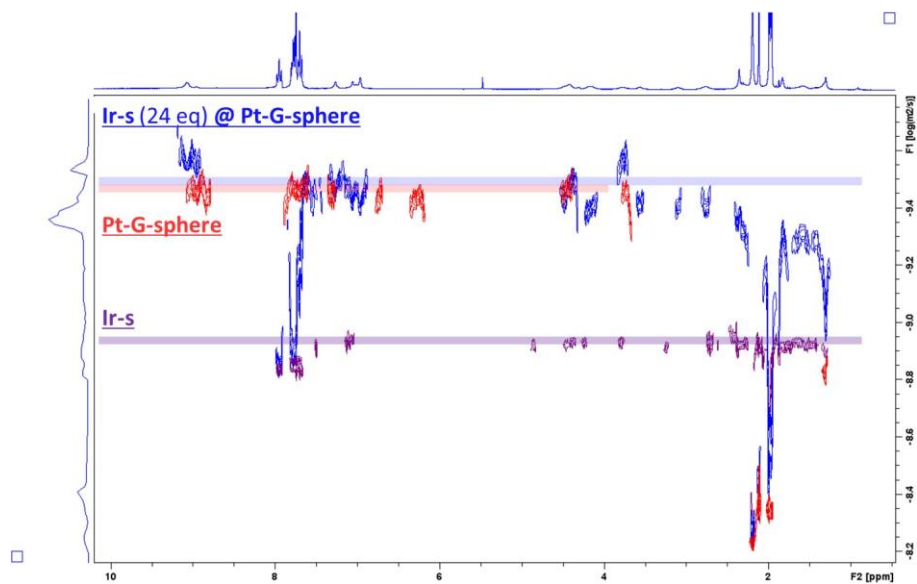


**Figure S39:** <sup>1</sup>H-DOSY-NMR spectrum of **Ir-s (24 eq) @ Pt-G-sphere** (blue) and reference spectra of **Ir-s** (purple) and **Pt-G-sphere** (red), all in CD<sub>3</sub>CN at 25°C (300 MHz)



# <sup>1</sup>H-NMR DOSY spectra of control groups

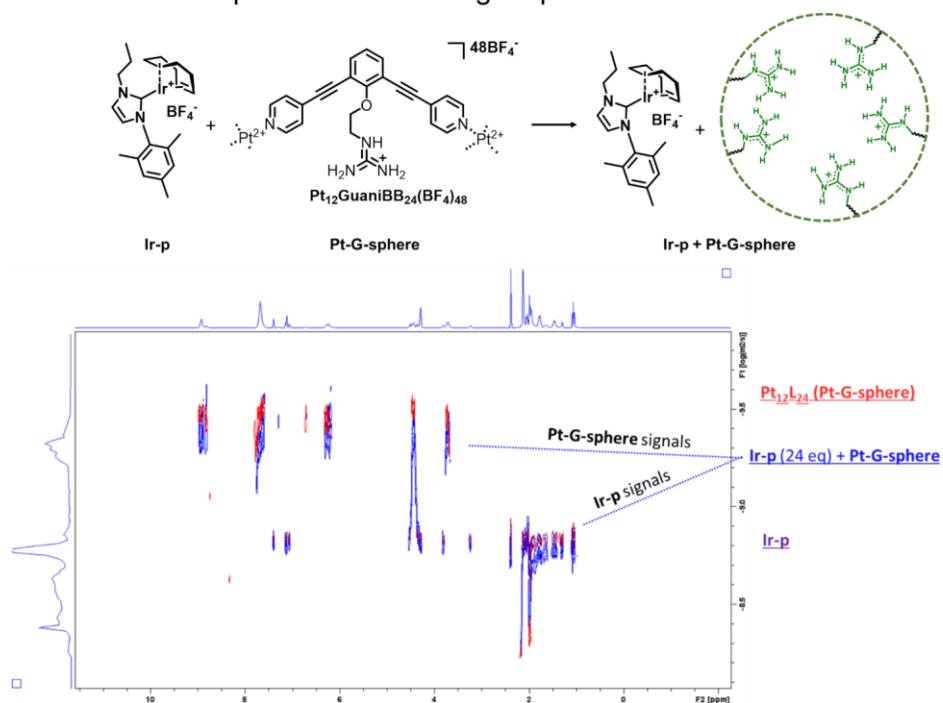


**Figure S40:** <sup>1</sup>H-DOSY-NMR spectrum of Ir-p (24 eq) + Pt-G-sphere (blue) and reference spectra of Ir-p (purple) and Pt-G-sphere (red), all in CD<sub>3</sub>CN at 25°C (300 MHz)

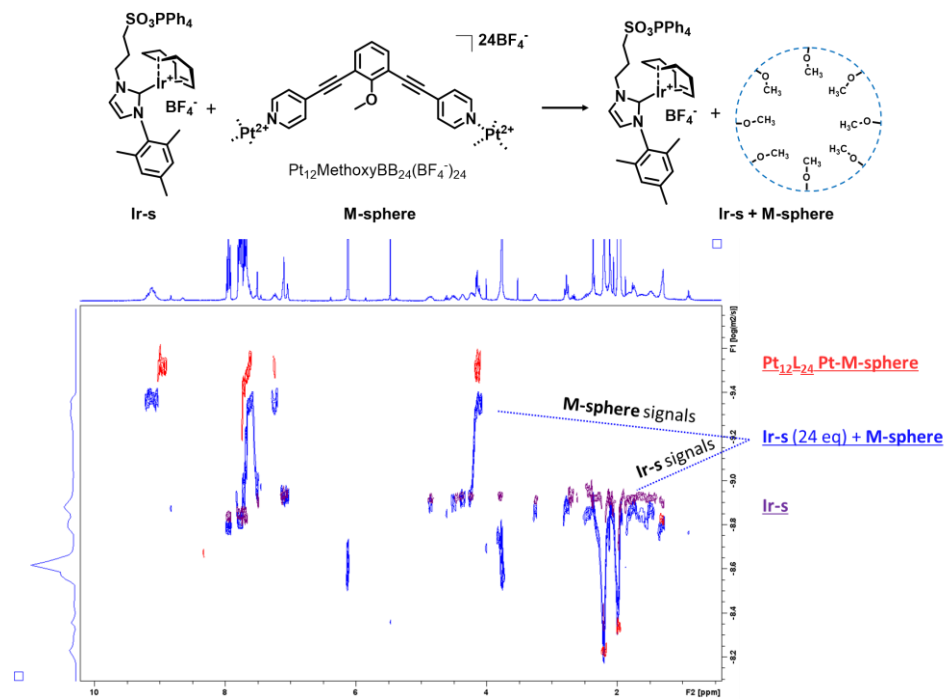


**Figure S41:**  $^1\text{H}$ -DOSY-NMR spectrum of **Ir-s + M-sphere** (blue) and reference spectra of **Ir-s** (purple) and **Pt-M-sphere** (red), all in  $\text{CD}_3\text{CN}$  at  $25^\circ\text{C}$  (300 MHz)

### Binding $^1\text{H}$ -NMR titration experiment

The binding behavior of Ir-s was further studied through  $^1\text{H}$ -NMR titration studies by following the N-H Guanidinium of the host (**Pt-G-sphere**) at varying guest (**Ir-s-BF<sub>4</sub>**) concentrations. These experiments were carried out under aerobic conditions. Two solutions (Host (A) and Host + Guest (B)) were prepared with equal [**Pt-G-sphere**] to ensure that adding guest to the Host solution would not result in interference with the observed shifts as a result of dilution.

### Titration with dilution correction

The volumes and concentrations of the corresponding solutions are described in the table below for the titration with dilution correction. Solution **A** contains only host and solution **B** contains host + guest (56 eq). 20  $\mu\text{L}$  portions of solution **B** were added to an NMR tube containing solution **A** and then vigorously shaken and measured after each step.

### Titration without dilution correction

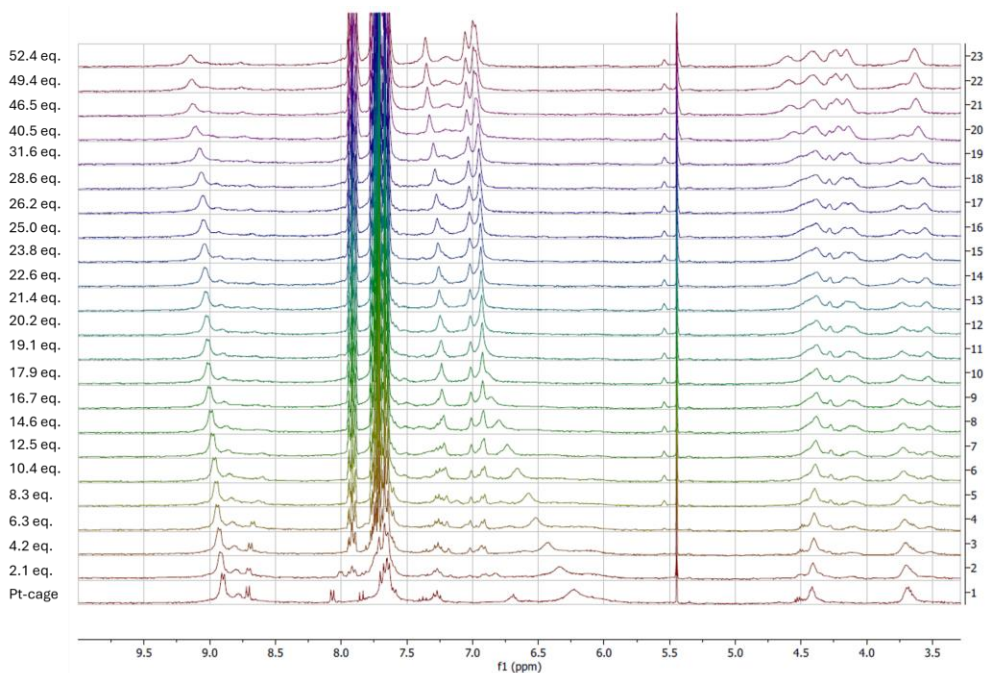
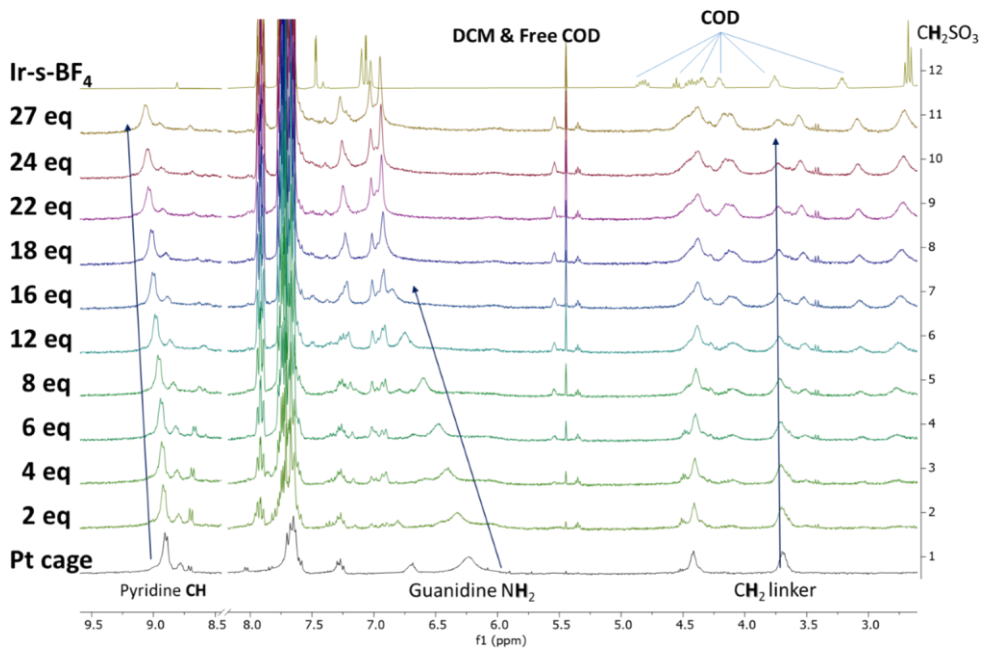
For the titration without dilution correction, the NMR tube was filled with a solution of **Pt-G-Sphere** (0.42 mM, 0.5 ml) and to this solution, a solution of **Ir-s-BF<sub>4</sub>** (0.63 mM) was added in small portions to obtain the shown equivalents (**Figure S42 - middle**).

As the relative guest concentration increases, the N-H signals of the guanidinium functional group strongly shift downfield, while the other signals remain relatively unaffected (**Figure S42 - top**). The shifts of the N-H signals were plotted against the corresponding guest / host ratios as depicted in **Figure S42 - bottom**.

**Table S1:** Dilution table, quantities and concentrations of the solutions used in the  $^1\text{H}$ -NMR titration experiment with dilution correction.

<b>Stock solutions</b>	mM				
[ <b>Pt-G-sphere</b> ] (sphere / BB)	0.42 / 10				
[ <b>Ir-s-BF<sub>4</sub></b> ]	62				
<b>Titration solutions</b>	<b>Pt-G-sphere</b> stock	<b>Ir-s</b> stock	CD3CN	[ <b>Pt-G-sphere</b> ] mM (sphere / BB)	[ <b>Ir-s</b> ] mM
<b>Solution A</b> (host)	0.4 ml	-	0.15 ml	0.3 / 7.3	0

<b>Solution B</b> (host + guest)	0.4 ml	0.15 ml	-	0.3 / 7.3	17
-------------------------------------	--------	---------	---	-----------	----



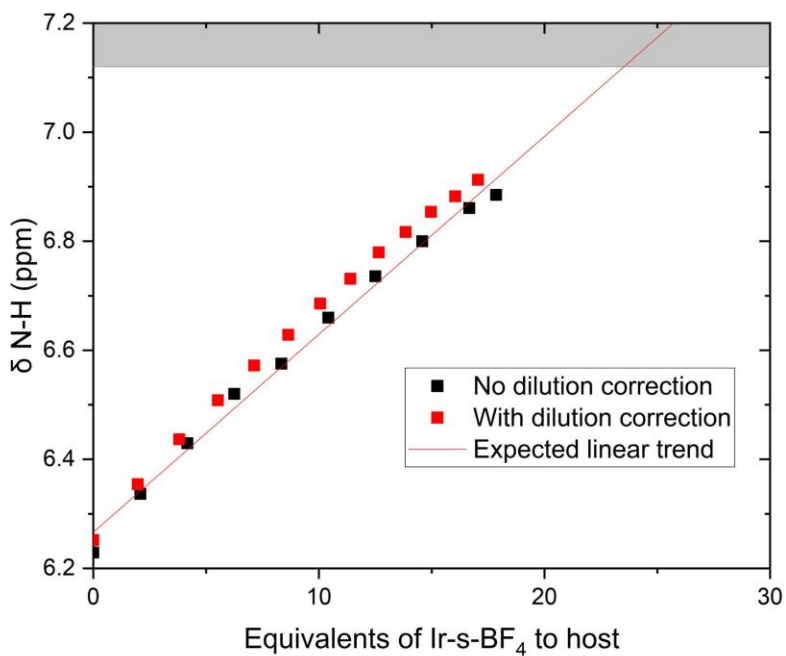


**Figure S42:** top: <sup>1</sup>H-NMR spectra of titration experiment **Ir-s-BF<sub>4</sub>** (x eq) @ **Pt-G-sphere** in CD<sub>3</sub>CN with dilution correction (300 MHz), middle: <sup>1</sup>H-NMR spectra of titration experiment **Ir-s-BF<sub>4</sub>** (x eq) @ **Pt-G-sphere** in CD<sub>3</sub>CN without dilution correction (300 MHz) bottom: <sup>1</sup>H-NMR titration **Ir-s** @ **Pt-G-sphere**, NH shift plotted against **Ir-s-BF<sub>4</sub>** : **G-sphere** ratio. Grey area shows ppm range where the N-H signal should be visible.

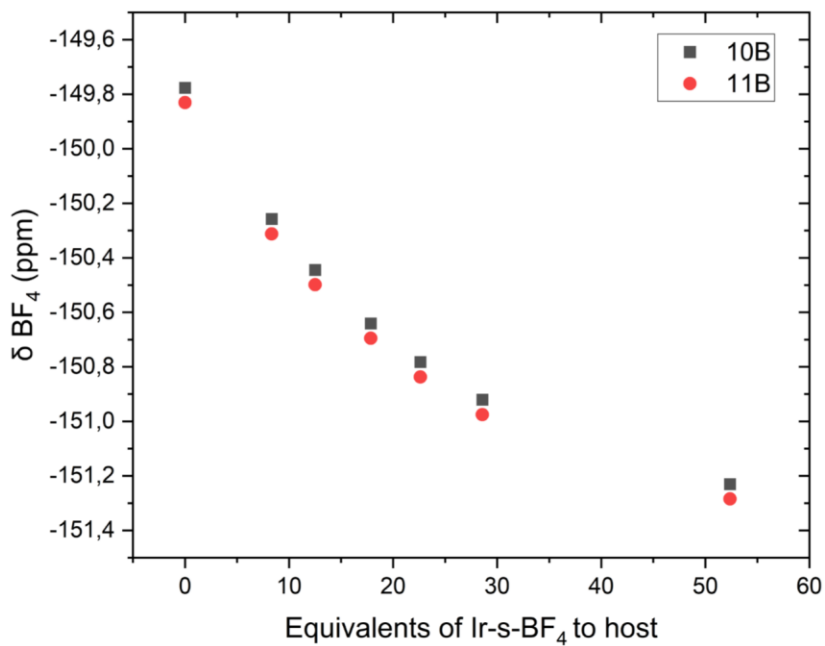
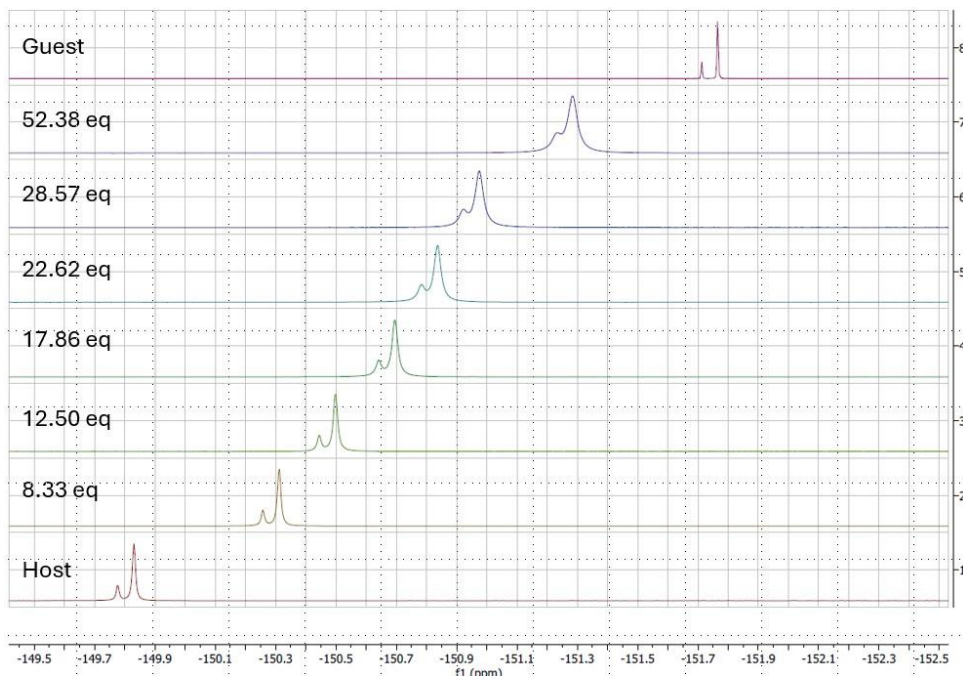


**Figure S43:** top:  $^{19}\text{F}$ -NMR spectra of titration experiment  $\text{Ir-s-BF}_4$  (x eq) @  $\text{Pt-G-sphere}$  in  $\text{CD}_3\text{CN}$  (300 MHz), bottom:  $^{19}\text{F}$ -NMR titration  $\text{Ir-s}$  @  $\text{Pt-G-sphere}$ ,  $\text{BF}_4$  shift plotted against  $\text{Ir-s-BF}_4$  :  $\text{G-sphere}$  ratio.

## MS-binding experiment

A sample of 8 eq **Ir-s @ Pd-G-sphere** was prepared by adding 16  $\mu\text{L}$  of a freshly prepared Ir-s solution in  $\text{CD}_3\text{CN}$  (63 mM, 0.5  $\mu\text{mol}$ ) to a **Pd-G-sphere** solution (0.3 ml, 0.42 mM,  $\mu\text{mol}$  0.125), after mixing, the solution was then further diluted and directly measured. The mass spectra were recorded as detailed in the general section of the SI.

In the mass spectrum (**Figure S44**), multiple charged species (6+ to 10+) corresponding to host guest combinations ranging from 5 – 9 equivalents of Ir-s are observed (**Figure S45**). These results are summarized in the **Table S2**. Additionally, as a result of ligand exchange and protonation and ligand hydrolysis under the MS conditions, these signals are accompanied by additional peaks (sometimes observed as broadened signals). The majority of these signals were identified as the addition of one or more imidazolium salt molecules (**S1**) or  $\text{H}_2\text{O}$ . As an example, the variations of **6 eq Ir-s @ Gsphere** + one imidazolium salt or  $\text{H}_2\text{O}$  molecule and **5 eq Ir-s @ G-sphere** + two imidazolium salt molecules are summarized in **Table S3** for multiple charged species (6 + to 10+) followed by a collection of overlays (**Figure S46 - 49**) to illustrate the peak broadening effect.

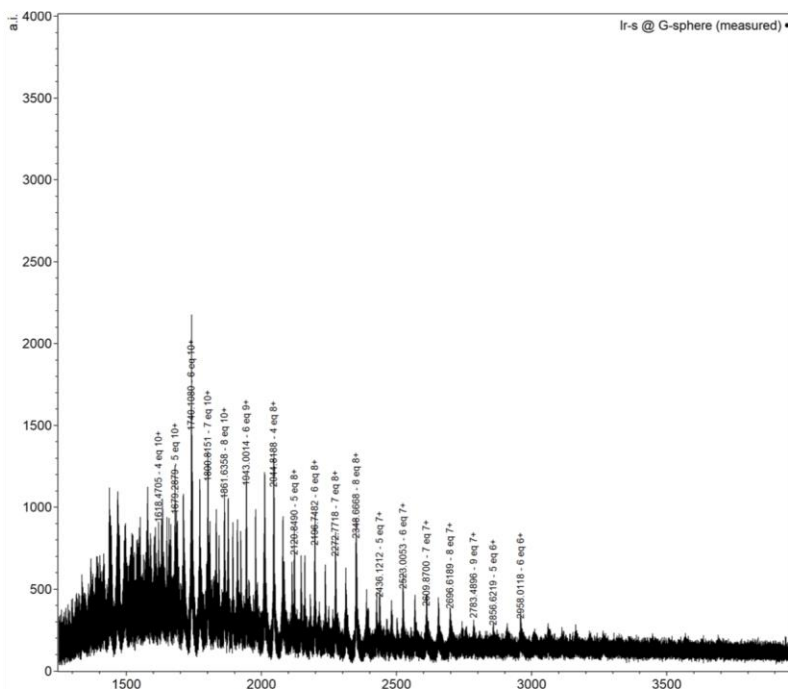


**Figure S44:** CSI-TOF mass spectrum (full spectrum) of the **Pd-G-sphere** ( $\text{Pd}_{12}\text{GuaniBB}_{24}$ )( $\text{BF}_4$ )<sub>48</sub> with 8 eq. **Ir-s** added, with a spray temperature of  $-40\text{ }^\circ\text{C}$  and a dry gas temperature of  $-35\text{ }^\circ\text{C}$ .

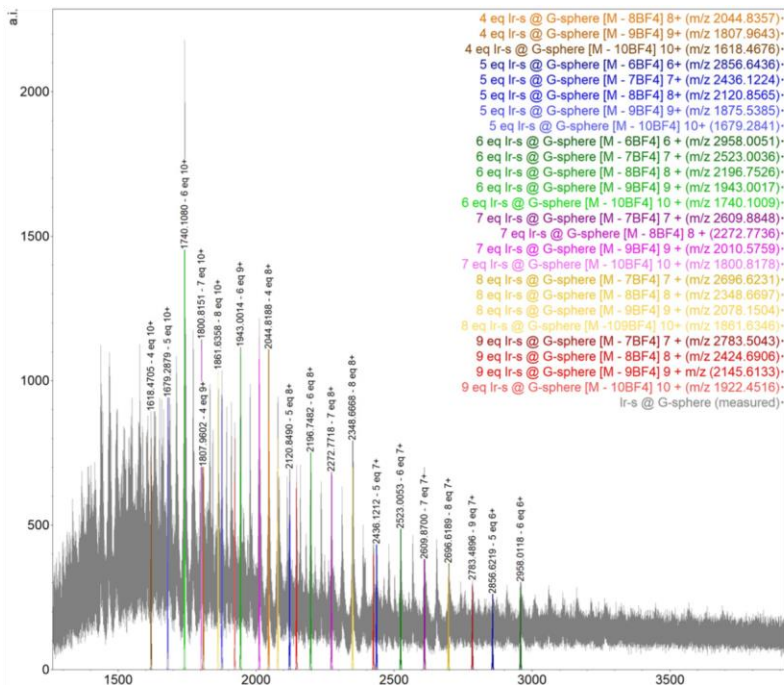


**Figure S45:** CSI-TOF mass spectrum (full spectrum) of the **Pd-G-sphere** ( $\text{Pd}_{12}\text{GuaniaBB}_{24}$ )( $\text{BF}_4$ )<sub>48</sub> with 8 eq. **Ir-s** added, with a spray temperature of  $-40^\circ\text{C}$  and a dry gas temperature of  $-35^\circ\text{C}$ , overlaid with simulated isotopic patterns in colour.

**Table S2:** Different charged species observed in the CSI-TOF mass spectrum of the **G-sphere** ( $\text{Pd}_{12}\text{GuaniaBB}_{24}$ )( $\text{BF}_4$ )<sub>48</sub> with 8 eq. **Ir-s-BF4** added and the corresponding found and calculated [m/z]. (Guest = [**Ir-s-BF4** -  $\text{BF}_4$  -  $\text{PPH}_4$ ])

z	Eq Ir-s	Species	Calc m/z	Found m/z
6 <sup>+</sup>	5 eq	$\text{Pd}_{12}\text{GuaniaBB}_{24}(\text{BF}_4)_{42}(\text{Guest})_5$	2856.6436	2856.6493
6 <sup>+</sup>	6 eq	$\text{Pd}_{12}\text{GuaniaBB}_{24}(\text{BF}_4)_{42}(\text{Guest})_6$	2958.0051	2958.0118

z	Eq Ir-s	Species	Calc m/z	Found m/z
7 <sup>+</sup>	5 eq	$\text{Pd}_{12}\text{GuaniaBB}_{24}(\text{BF}_4)_{41}(\text{Guest})_5$	2436.1224	2436.1212
7 <sup>+</sup>	6 eq	$\text{Pd}_{12}\text{GuaniaBB}_{24}(\text{BF}_4)_{41}(\text{Guest})_6$	2523.0036	2523.0053
7 <sup>+</sup>	7 eq	$\text{Pd}_{12}\text{GuaniaBB}_{24}(\text{BF}_4)_{41}(\text{Guest})_7$	2609.8848	2609.8700
7 <sup>+</sup>	8 eq	$\text{Pd}_{12}\text{GuaniaBB}_{24}(\text{BF}_4)_{41}(\text{Guest})_8$	2696.6231	2696.6189
7 <sup>+</sup>	9 eq	$\text{Pd}_{12}\text{GuaniaBB}_{24}(\text{BF}_4)_{41}(\text{Guest})_9$	2783.5043	2783.4896

z	eq Ir-s	Species	Calc m/z	Found m/z
8 <sup>+</sup>	4 eq	$\text{Pd}_{12}\text{GuaniaBB}_{24}(\text{BF}_4)_{40}(\text{Guest})_4$	2044.8357	2044.8188
8 <sup>+</sup>	5 eq	$\text{Pd}_{12}\text{GuaniaBB}_{24}(\text{BF}_4)_{40}(\text{Guest})_5$	2120.7315	2120.7270

8 <sup>+</sup>	6 eq	Pd12 <b>GuaniBB</b> 24(BF4)40( <b>Guest</b> )6	2197.2561	2197.2516
8 <sup>+</sup>	7 eq	Pd12 <b>GuaniBB</b> 24(BF4)40( <b>Guest</b> )7	2272.7736	2272.7718
8 <sup>+</sup>	8eq	Pd12 <b>GuaniBB</b> 24(BF4)40( <b>Guest</b> )8	2348.6697	2348.6668
8 <sup>+</sup>	9 eq	Pd12 <b>GuaniBB</b> 24(BF4)40( <b>Guest</b> )9	2424.6906	2424.6872

<b>z</b>	<b>eq lr-s</b>	<b>molecular code</b>	<b>Calc m/z</b>	<b>Found m/z</b>
9 <sup>+</sup>	4 eq	Pd12 <b>GuaniBB</b> 24(BF4)39( <b>Guest</b> )4	1740.5013	1740.5042
9 <sup>+</sup>	5 eq	Pd12 <b>GuaniBB</b> 24(BF4)39( <b>Guest</b> )5	1875.5385	1875.5382
9 <sup>+</sup>	6 eq	Pd12 <b>GuaniBB</b> 24(BF4)39( <b>Guest</b> )6	1943.0017	1943.0014
9 <sup>+</sup>	7 eq	Pd12 <b>GuaniBB</b> 24(BF4)39( <b>Guest</b> )7	2010.5759	2010.5766
9 <sup>+</sup>	8eq	Pd12 <b>GuaniBB</b> 24(BF4)39( <b>Guest</b> )8	2078.1504	2078.1528
9 <sup>+</sup>	9 eq	Pd12 <b>GuaniBB</b> 24(BF4)39( <b>Guest</b> )9	2145.6133	2145.6140

<b>z</b>	<b>eq lr-s</b>	<b>molecular code</b>	<b>Calc m/z</b>	<b>Found m/z</b>
10 <sup>+</sup>	5 eq	Pd12 <b>GuaniBB</b> 24(BF4)38( <b>Guest</b> )5	1679.2841	1679.2879
10 <sup>+</sup>	6 eq	Pd12 <b>GuaniBB</b> 24(BF4)38( <b>Guest</b> )6	1740.1009	1740.1080
10 <sup>+</sup>	7 eq	Pd12 <b>GuaniBB</b> 24(BF4)38( <b>Guest</b> )7	1800.8178	1800.8151
10 <sup>+</sup>	8eq	Pd12 <b>GuaniBB</b> 24(BF4)38( <b>Guest</b> )8	1861.6346	1861.6358
10 <sup>+</sup>	9 eq	Pd12 <b>GuaniBB</b> 24(BF4)38( <b>Guest</b> )9	1922.4516	1922.4493



<b>z</b>	<b>Eq Ir-s</b>	<b>Species</b>	<b>Calc m/z</b>	<b>Found m/z</b>
6 <sup>+</sup>	6	Pd <sub>12</sub> GuaniBB <sub>24</sub> (BF <sub>4</sub> ) <sub>42</sub> (Guest) <sub>6</sub> (S1)		
6 <sup>+</sup>	6	Pd <sub>12</sub> GuaniBB <sub>24</sub> (BF <sub>4</sub> ) <sub>42</sub> (Guest) <sub>6</sub> (S1)(OH)		
6 <sup>+</sup>	6	Pd <sub>12</sub> GuaniBB <sub>24</sub> (BF <sub>4</sub> ) <sub>42</sub> (Guest) <sub>6</sub> (H <sub>2</sub> O)		
<b>Table S3:</b> Different charged species observed in the CSI-TOF mass spectrum of variations of ligand (S1) and/or water additions the G-sphere (Pd <sub>12</sub> GuaniBB <sub>24</sub> BF <sub>4</sub> ) <sub>48</sub> with 8 eq. Ir-s-BF <sub>4</sub> added and the corresponding found and calculated [m/z]. This table is as an example with 6 eq Ir-s (Guest = [Ir-s-BF <sub>4</sub> – BF <sub>4</sub> – PPh <sub>4</sub> ])			3009.3583	3009.3501
			3012.1922	3012.1794
			2961.0069	2961.0220
			2959.5170	2959.5019
<b>z</b>	<b>eq Ir-s</b>	<b>Species</b>	<b>Calc m/z</b>	<b>Found m/z</b>
7 <sup>+</sup>	6	Pd <sub>12</sub> GuaniBB <sub>24</sub> (BF <sub>4</sub> ) <sub>41</sub> (Guest) <sub>6</sub> (S1)		
7 <sup>+</sup>	6	Pd <sub>12</sub> GuaniBB <sub>24</sub> (BF <sub>4</sub> ) <sub>41</sub> (Guest) <sub>6</sub> (S1)(OH)		
7 <sup>+</sup>	6	Pd <sub>12</sub> GuaniBB <sub>24</sub> (BF <sub>4</sub> ) <sub>41</sub> (Guest) <sub>6</sub> (H <sub>2</sub> O)		
6 <sup>+</sup>	5	Pd <sub>12</sub> GuaniBB <sub>24</sub> (BF <sub>4</sub> ) <sub>42</sub> (Guest) <sub>5</sub> (S1) <sub>2</sub>	2567.0208	2567.0111
			2569.4498	2569.4343
			2525.5765	2525.5763
			2524.2997	2524.2859
<b>z</b>	<b>eq Ir-s</b>	<b>Species</b>	<b>Calc m/z</b>	<b>Found m/z</b>
8 <sup>+</sup>	6	Pd <sub>12</sub> GuaniBB <sub>24</sub> (BF <sub>4</sub> ) <sub>40</sub> (Guest) <sub>6</sub> (S1)		
8 <sup>+</sup>	6	Pd <sub>12</sub> GuaniBB <sub>24</sub> (BF <sub>4</sub> ) <sub>40</sub> (Guest) <sub>6</sub> (S1)(OH)		
8 <sup>+</sup>	6	Pd <sub>12</sub> GuaniBB <sub>24</sub> (BF <sub>4</sub> ) <sub>40</sub> (Guest) <sub>6</sub> (H <sub>2</sub> O)		
			2235.2675	2235.2655
			2237.3930	2237.3914
			2199.0038	2199.0057
			2197.8866	2197.8774
7 <sup>+</sup>	5	Pd <sub>12</sub> GuaniBB <sub>24</sub> (BF <sub>4</sub> ) <sub>41</sub> (Guest) <sub>5</sub> (S1) <sub>2</sub>		
8 <sup>+</sup>	5	Pd <sub>12</sub> GuaniBB <sub>24</sub> (BF <sub>4</sub> ) <sub>40</sub> (Guest) <sub>5</sub> (S1) <sub>2</sub>		

<b>z</b>	<b>eq</b>	<b>Species</b>	<b>Calc m/z</b>	<b>Found m/z</b>
9 <sup>+</sup>	6	Pd <sub>12</sub> <b>GuaniBB</b> <sub>24</sub> (BF <sub>4</sub> ) <sub>39</sub> ( <b>Guest</b> ) <sub>6</sub> ( <b>S1</b> )		
9 <sup>+</sup>	6	Pd <sub>12</sub> <b>GuaniBB</b> <sub>24</sub> (BF <sub>4</sub> ) <sub>39</sub> ( <b>Guest</b> ) <sub>6</sub> ( <b>S1</b> )(OH)		
9 <sup>+</sup>	6	Pd <sub>12</sub> <b>GuaniBB</b> <sub>24</sub> (BF <sub>4</sub> ) <sub>39</sub> ( <b>Guest</b> ) <sub>6</sub> (H <sub>2</sub> O)		
9 <sup>+</sup>	5	Pd <sub>12</sub> <b>GuaniBB</b> <sub>24</sub> (BF <sub>4</sub> ) <sub>39</sub> ( <b>Guest</b> ) <sub>5</sub> (S1) <sub>2</sub>	1977.3483	1977.3481
			1979.2378	1979.2345
			1945.0029	1945.0054
			1944.0099	1944.0001

<b>z</b>	<b>eq</b>	<b>Species</b>	<b>Calc m/z</b>	<b>Found m/z</b>
10 <sup>+</sup>	6	Pd <sub>12</sub> <b>GuaniBB</b> <sub>24</sub> (BF <sub>4</sub> ) <sub>38</sub> ( <b>Guest</b> ) <sub>6</sub> ( <b>S1</b> )		
10 <sup>+</sup>	6	Pd <sub>12</sub> <b>GuaniBB</b> <sub>24</sub> (BF <sub>4</sub> ) <sub>38</sub> ( <b>Guest</b> ) <sub>6</sub> ( <b>S1</b> )(OH)	1770.9147	1770.9147
			1772.6136	1772.6097
			1741.9020	1741.9028
			1740.9084	1740.9040
10 <sup>+</sup>	6	Pd <sub>12</sub> <b>GuaniBB</b> <sub>24</sub> (BF <sub>4</sub> ) <sub>38</sub> ( <b>Guest</b> ) <sub>6</sub> (H <sub>2</sub> O)		
10 <sup>+</sup>	5	Pd <sub>12</sub> <b>GuaniBB</b> <sub>24</sub> (BF <sub>4</sub> ) <sub>38</sub> ( <b>Guest</b> ) <sub>5</sub> (S1) <sub>2</sub>		

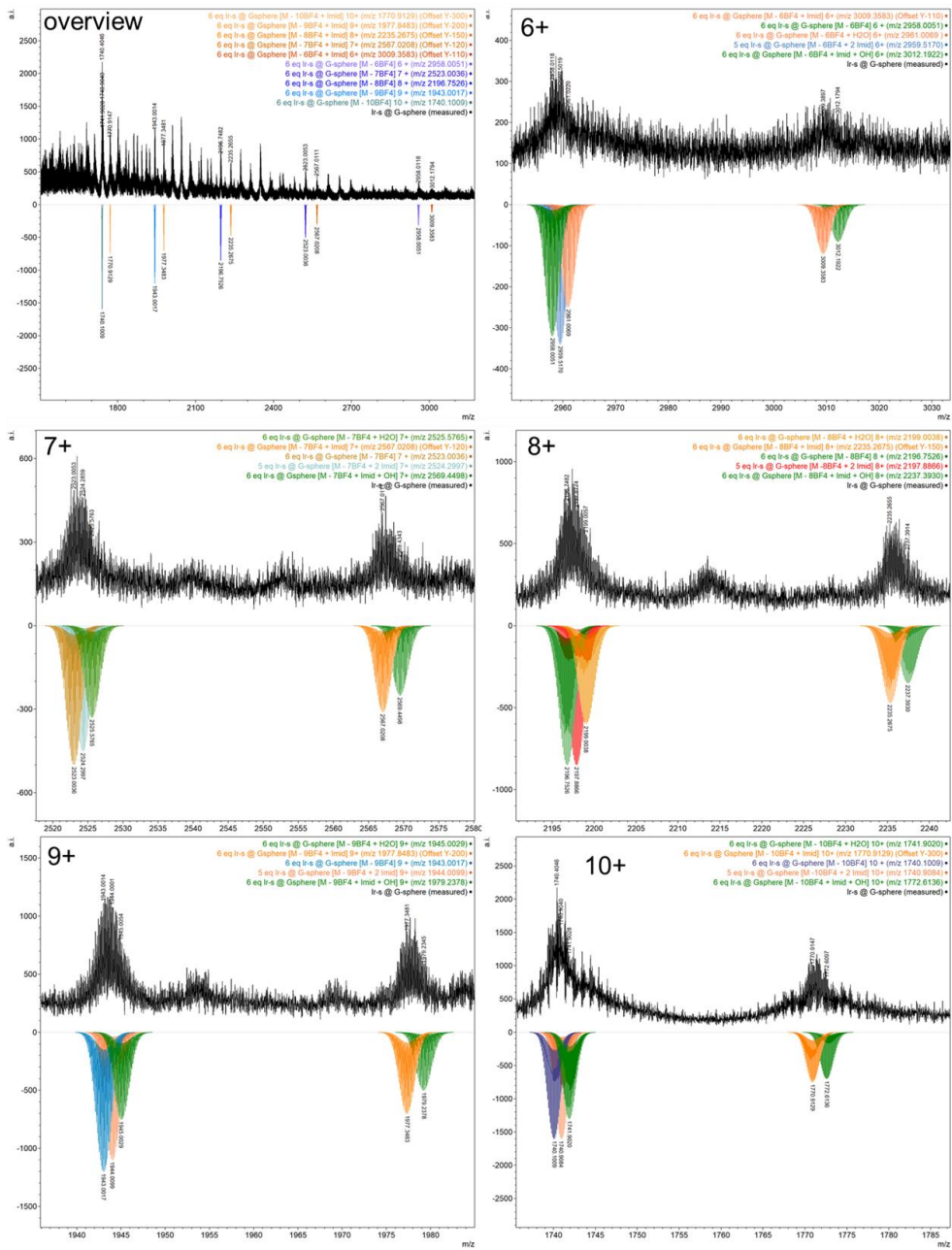


**Figure S46:** CSI-TOF mass spectrum, zoomed spectra of differently charged species of the of the Pd-Gsphere (Pd<sub>12</sub>GuanibB<sub>24</sub>)(BF<sub>4</sub>)<sub>48</sub> with 8 eq. Ir-s added and their variations of different amounts of ligand or water added. With a spray temperature of  $-40$  °C and a dry gas temperature of  $-35$  °C, overlaid with simulated isotopic patterns in colour. (starting top left with an overview followed by charges 6+ to 10+)

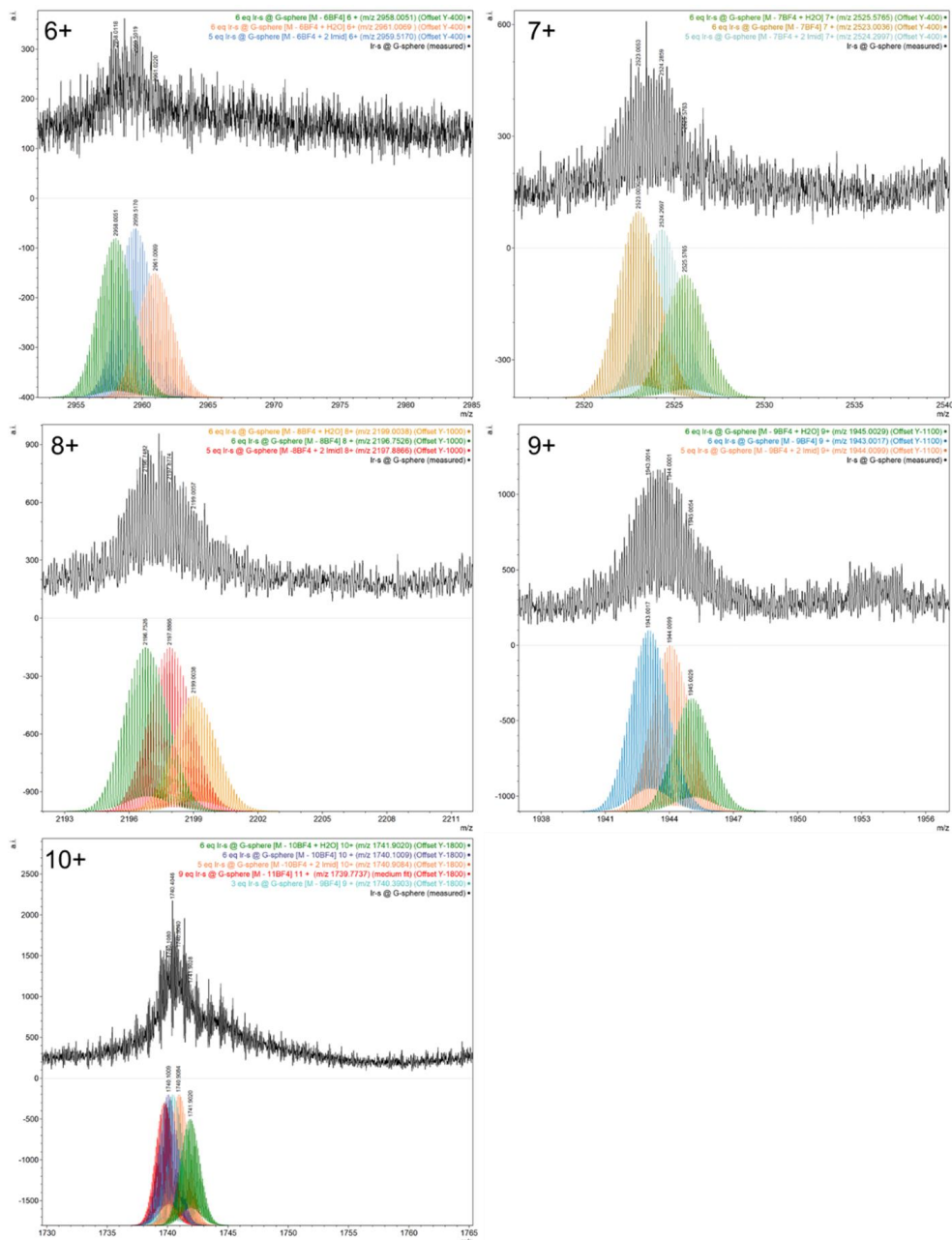


**Figure S47:** CSI-TOF mass spectrum, zoomed spectra of differently charged species of the of the **Pd-Gsphere** ( $\text{Pd}_{12}\text{GuaniBB}_{24}$ )( $\text{BF}_4$ )<sub>48</sub> with 8 eq. Ir-s added and variations of different amounts of ligand (S1) or water added focussed on the broadened peaks. With a spray temperature of  $-40^\circ\text{C}$  and a dry gas temperature of  $-35^\circ\text{C}$ , overlaid with simulated isotopic patterns in colour of charges 6- to 10+.

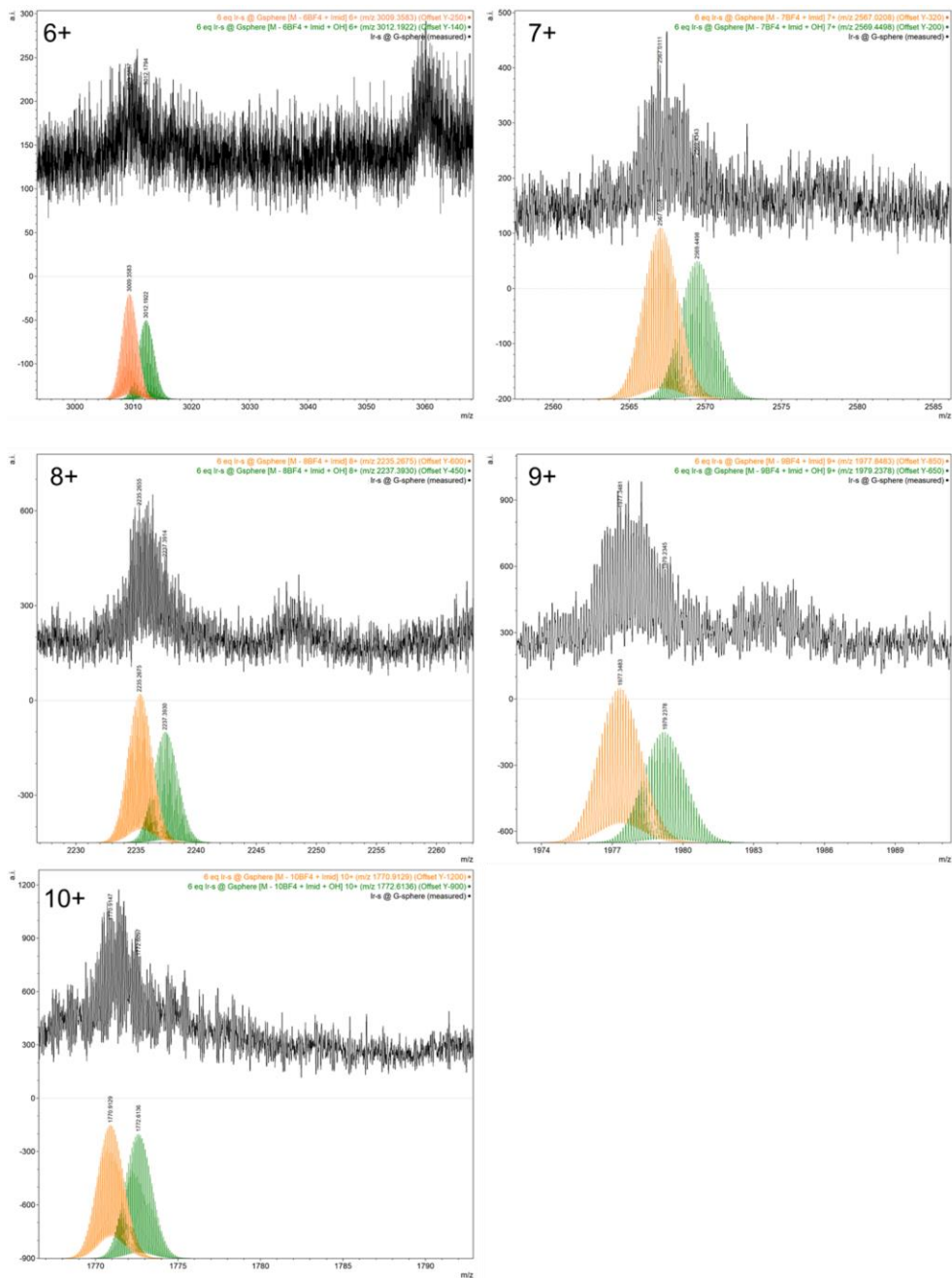


**Figure S48:** CSI-TOF mass spectrum, zoomed spectra of differently charged species of the of the **Pd-Gsphere** ( $\text{Pd}_{12}\text{GuaniBB}_{24}$ )( $\text{BF}_4$ )<sub>48</sub> with 8 eq. **Ir-s** added and one imidazolium ligand (**S1**) (+ water added). With a spray temperature of  $-40^\circ\text{C}$  and a dry gas temperature of  $-35^\circ\text{C}$ , overlaid with simulated isotopic patterns in colour of charges 6+ to 10+

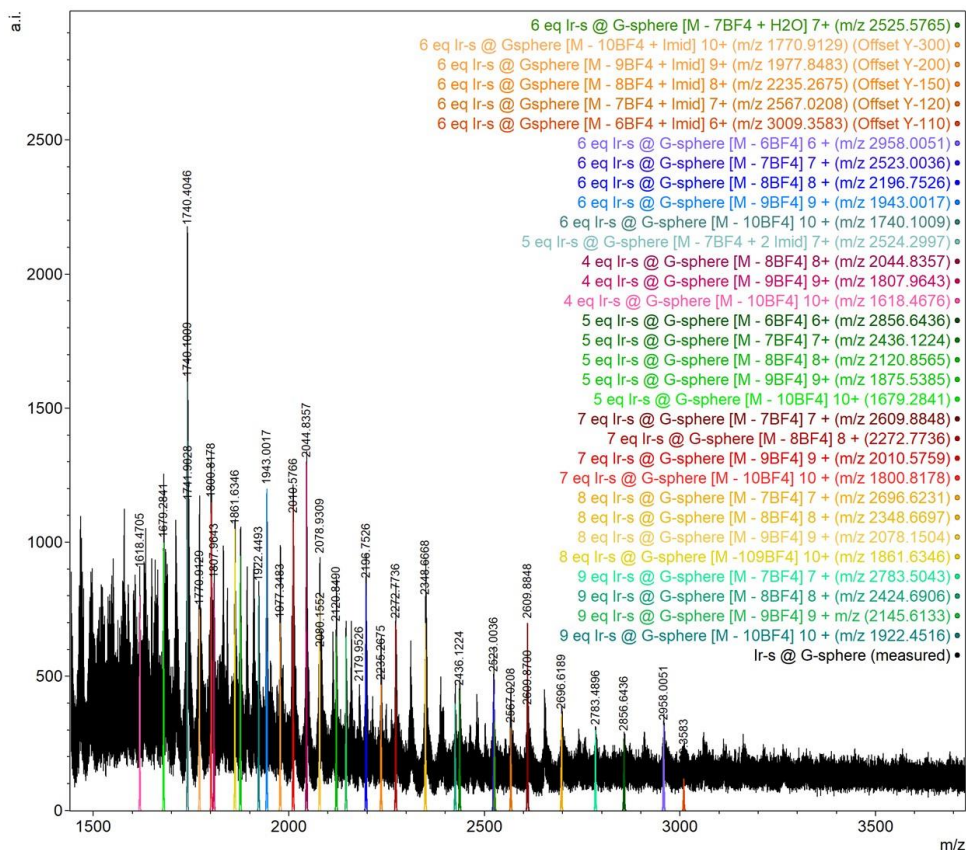


**Figure S49:** CSI-TOF mass spectrum (full spectrum) of the **Pd-G-sphere** (Pd<sub>12</sub>GuaniBB<sub>24</sub>)(BF<sub>4</sub>)<sub>48</sub> with 8 eq. **Ir-s** added, with a spray temperature of  $-40\text{ }^{\circ}\text{C}$  and a dry gas temperature of  $-35\text{ }^{\circ}\text{C}$ , overlaid with simulated isotopic patterns in colour, all expected peaks including the 6eq **Ir-s** + **S1** @ **Pd-G-sphere** signals.

## Nanocluster synthesis

### Synthesis of Ir-s @ G-sphere\*:

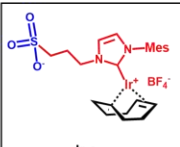
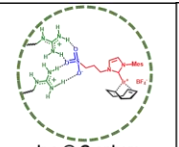
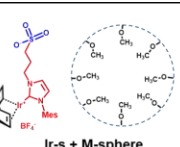
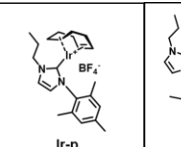
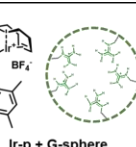










(Representative procedure for the nanoparticle synthesis)

1 ml **Pt-G-sphere** solution (1 ml, 0.42 mM, 0.42  $\mu\text{mol}$  sphere) was moved to a 4 ml vial equipped with a stirring bean in an Argon bucket. Then, 0.160 ml of freshly prepared **Ir-s-BF<sub>4</sub>** solution in CD<sub>3</sub>CN (62.6 mM, 10  $\mu\text{mol}$ , 24 eq) was added to the stirring **Pt-G-sphere** solution with a micropipette under Argon flow. The resulting light orange solution was capped and allowed to mix for 10 min. Then the vial was moved to an Argon purged autoclave and the vial was equipped with a needle. Thereafter, the autoclave was pressurized with 50 bar H<sub>2</sub>, placed in a preheated oil bath (50  $^{\circ}\text{C}$ ) and stirred at 800 rpm. After 18h, the autoclave was cooled with an ice bath and slowly de-pressurized.

The resulting red/brown particle solution was transferred to and stored under Argon atmosphere and used without further purification.

#### Synthesis of the control samples:

The control samples were prepared in an identical fashion, with 0.160 ml of metal precursor solution (**Ir-s-BF<sub>4</sub>** or **Ir-p-BF<sub>4</sub>**, both 62.6 mM) and either 1 ml sphere (**Pt-G-sphere** or **M-sphere** both 0.42 mM) or 1 ml CD<sub>3</sub>CN (in the case of controls without the sphere).

	 Ir-s	 Ir-s @ G-sphere	 Ir-s + M-sphere	 Ir-p	 Ir-p + G-sphere
	No nanosphere (SO <sub>3</sub> )	Particle @ nanosphere	Non-encapsulated (SO <sub>3</sub> + nanosphere)	No nanosphere (aliphatic)	Non-encapsulated (Guanidinium + aliphatic)
Before					
After					

**Figure S50:** Representative photos of precursor/nanosphere solutions before and after hydrogenation for the synthesis of **Ir-s @ G-sphere\*** and the control groups

#### Synthesis of Ir @ PVP:

The Ir @ PVP was synthesized according to a literature protocol.<sup>14</sup> H<sub>2</sub>IrCl<sub>6</sub> (0.1 mmol) and PVP (2.0 mmol, K30, MW = 40 kDa) were dissolved in H<sub>2</sub>O (40 ml) and an aqueous solution of NaBH<sub>4</sub> (5.0 mmol, 5 ml) was added to the Ir-solution at room temperature while bubbling argon gas through the Ir-solution. After immediate color change from brown to yellow, the solution was stirred for 6h as it slowly turned dark brown. The solution was passed through a membrane filter (MWCO 3 kDa) and was washed with D<sub>2</sub>O (3 x 10 ml) to make the solution suitable for NMR experiments. The integrals of the PVP against 1,3,5-trimethoxybenzene in a CD<sub>3</sub>CN/D<sub>2</sub>O (1/1) solution were used to determine the concentration of Ir.

**Table S4:** Quantification of the encapsulated **Ir-s-BF<sub>4</sub>** complex before hydrogenation and the amount of cyclooctane (**COT**) formed after hydrogenation. Based on <sup>1</sup>H-NMR integrals and internal standard (IS, 1,3,5-trimethoxybenzene) in spectra found in Figure S44 and Figure S45.

	<b>Integrated peak</b>	<b>Integral vs IS</b>	<b>[IS]</b>	<b>[ component ]</b>	<b>component</b>
<b>Before</b>	<b>CH<sub>2</sub>-SO<sub>3</sub>: 2.73 ppm</b>	0.46	0.027	6.18 mM	Ir-s-BF <sub>4</sub>
<b>After</b>	<b>COT: 1.54 ppm</b>	3.71	0.029	6.21 mM	COT



---

TEM images of control groups

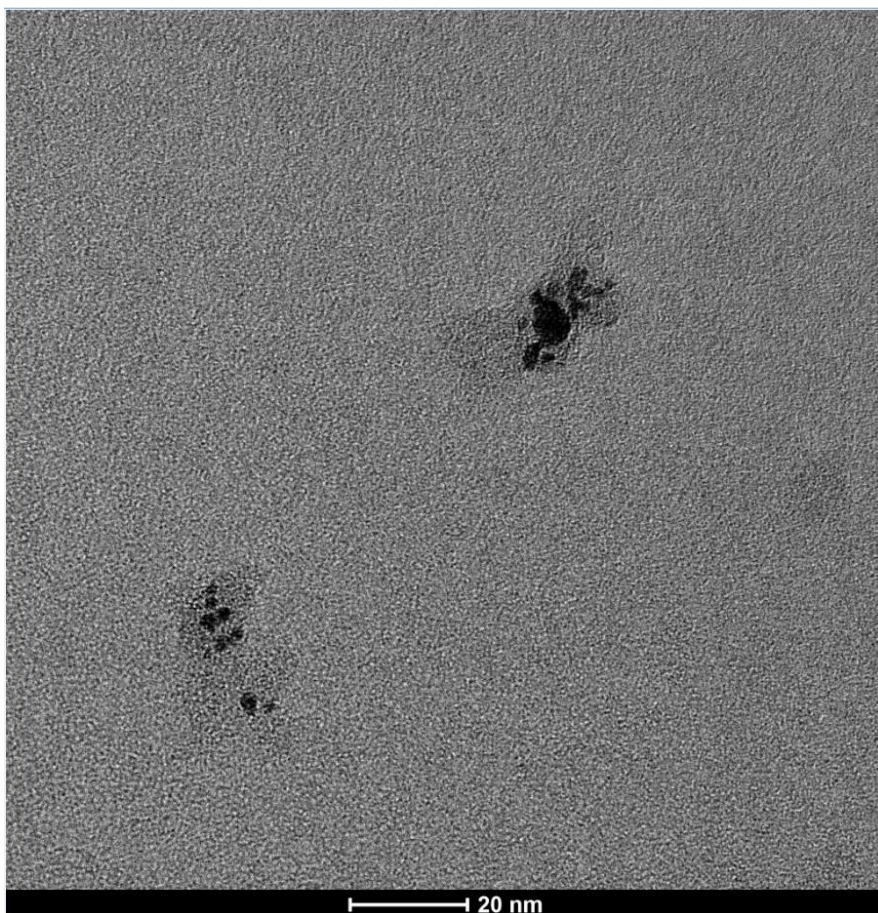


**Figure S51: Representative TEM image of Ir-s + M-sphere\***



Figure S52: Representative TEM image of Ir-p + G-sphere\*

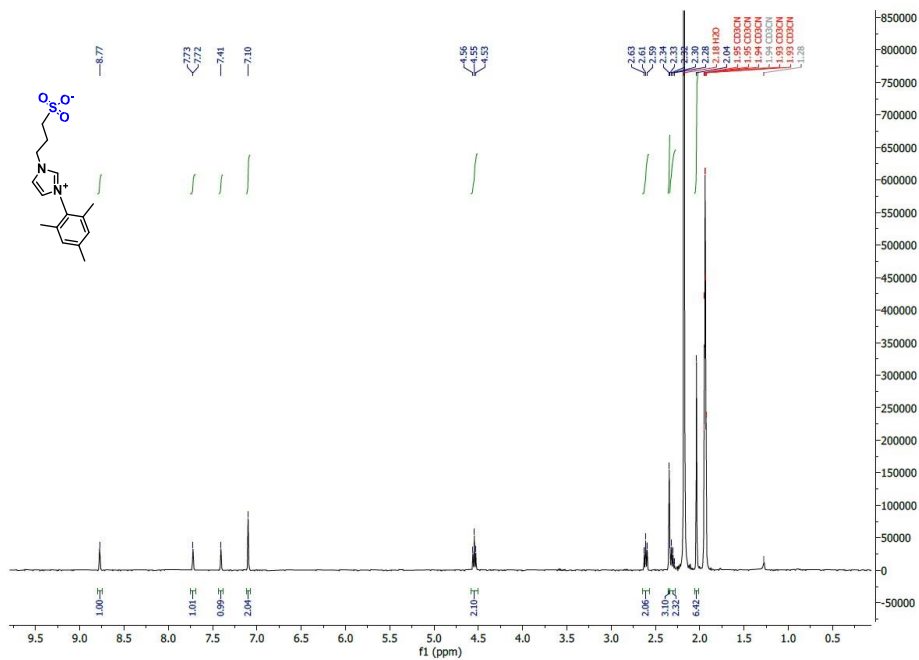


Figure S53: <sup>1</sup>H-NMR spectrum of Mes-Imid-s (in CD<sub>3</sub>CN, 400 MHz).

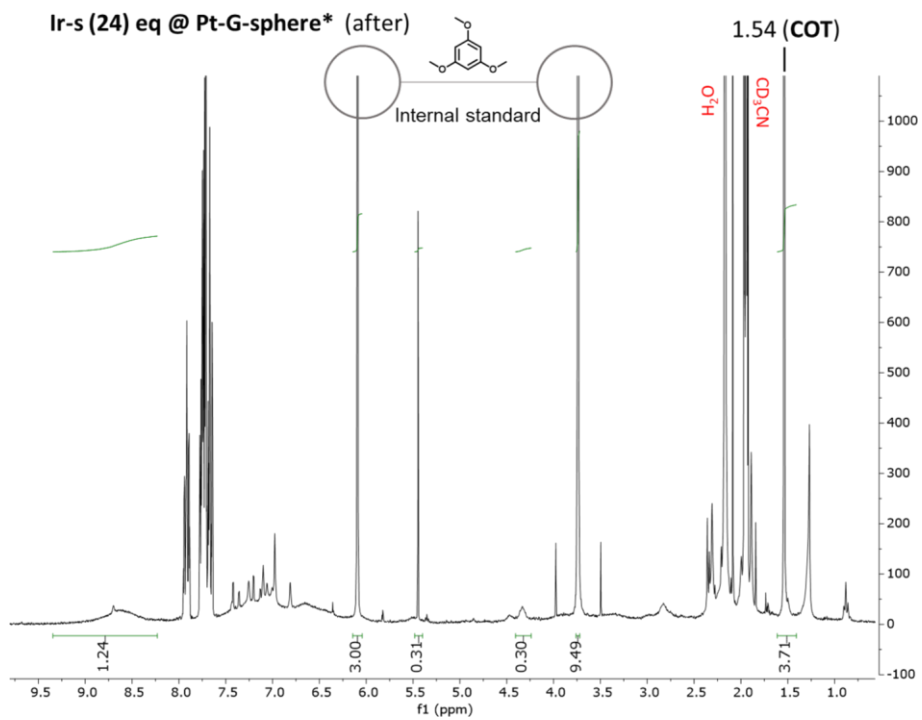
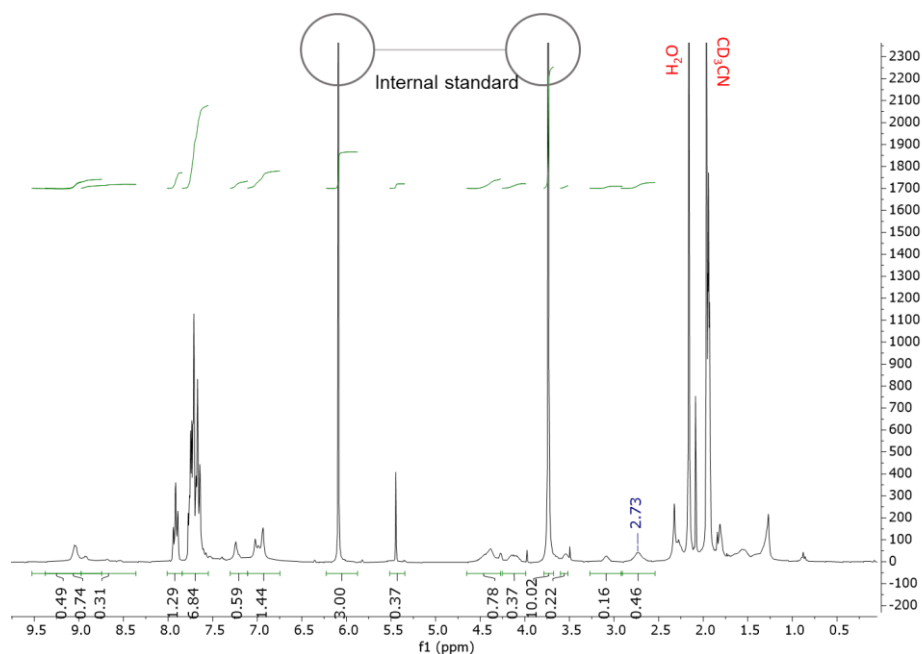


Figure S54: <sup>1</sup>H-NMR spectrum of Ir-s (24 eq) @ Pt-G-sphere\* in the presence of an internal standard (1,3,5-trimethoxybenzene) after hydrogenation (in CD<sub>3</sub>CN, 300 MHz)



**Figure S55:**  $^1\text{H-NMR}$  spectrum of Ir-s (24 eq) @ Pt-G-sphere in the presence of an internal standard (1,3,5-trimethoxybenzene) before hydrogenation (in  $\text{CD}_3\text{CN}$ , 300 MHz)

### ICP-OES of Ir-s @ G-sphere

**Table S5:** Found values for ICP-OES measurements of Ir-s @ G-sphere\* as prepared and relative mol%, corresponding to a 24:12 Ir : Pt ratio.

	Ir	Pt	mol%
Ir	0.098	0.509	66%
Pt	0.050	0.259	34%

Catalysis: General procedure of the catalytic tests over time

The catalytic tests with Ir-s @ G-sphere\*, Ir-s + M-sphere\* at different time stamps were all performed as stated below. For each time stamp, separate samples were prepared to avoid any disruptions or air contamination during the process.

Under an inert atmosphere, 0.42 ml of stock solution containing 4nitrostyrene\*\* (1) (80 mM, 32  $\mu\text{mol}$ ) and dodecane (0.33 mM, 0.14  $\mu\text{mol}$ ) in  $\text{CH}_3\text{CN}$  was added to a 2 ml vial equipped with a stirring bean. Then 80  $\mu\text{L}$  of an as prepared nanoparticle solution (8.63 mM, 1.38  $\mu\text{mol}$ , 2 mol% vs 1) was added to the vial containing the stock solution. The resulting solution was mixed and a sample was taken. Then the vials were capped and moved to an

Argon purged autoclave and equipped with a needle. The sealed autoclave was pressurized with H<sub>2</sub> (50 bar) and placed in a preheated oil bath (50 °C) and stirred (800 rpm) for x hours. After x hours, the autoclave was cooled with ice and depressurized and samples were immediately taken and diluted with 2-propanol and quantified by GC-MS analysis.

\*\*A fresh bottle of 4-nitrostyrene (STREM chemicals) was filtered over hot activated alumina prior to use.

---

#### Catalysis: General procedure of High-Pressure NMR experiments

**NOTE:** When performing high-pressure experiments one should take appropriate safety measures. The tube should be handled as a small explosive device. The scientist should never be directly exposed to a pressurized tube. Pressurizing and handling the tube should be done behind a polycarbonate protective shield. The individual scientist should verify that the safety requirements are met and that the equipment is in good condition.

The catalytic tests with **Ir-s @ G-sphere\*** and **Ir @ PVP** by means of high pressure NMR were done as stated below. At room temperature, the reaction does not start and there is no evident H<sub>2</sub> peak visible.

Under an inert atmosphere, 0.42 ml of stock solution containing styrene\*\* (80 mM, 32 μmol), Et<sub>3</sub>N (8 mM, 3.2 μmol)\*\*\*, and dodecane (0.33 mM, 0.14 μmol) in CD<sub>3</sub>CN was added to a flame dried schlenk and deoxygenated by three freeze-pump-thaw cycles. Then, 80 μL of an as prepared nanoparticle solution (8.63 mM, 1.38 μmol, 2 mol% vs styrene) was added to the schlenk containing the stock solution. The resulting solution was mixed and added to a sapphire NMR tube under a flow of Argon.<sup>15</sup> The tube was closed, and was pressurized with H<sub>2</sub> (40 bar) and heated in the NMR machine to 50°C. As soon as the temperature reached 50°C, an <sup>1</sup>H-NMR spectrum was recorded (this is used as t = 0) and then, an <sup>1</sup>H-NMR measurement was taken every hour. After reaction completion, the temperature was cooled to room temperature and the NMR tube was removed and depressurized in a fume hood.

\*\*Styrenes were filtered over basic alumina prior to use.

\*\*\* Et<sub>3</sub>N (10 mol%) was used as base to deprotonate 3-vinylbenzoic acid.

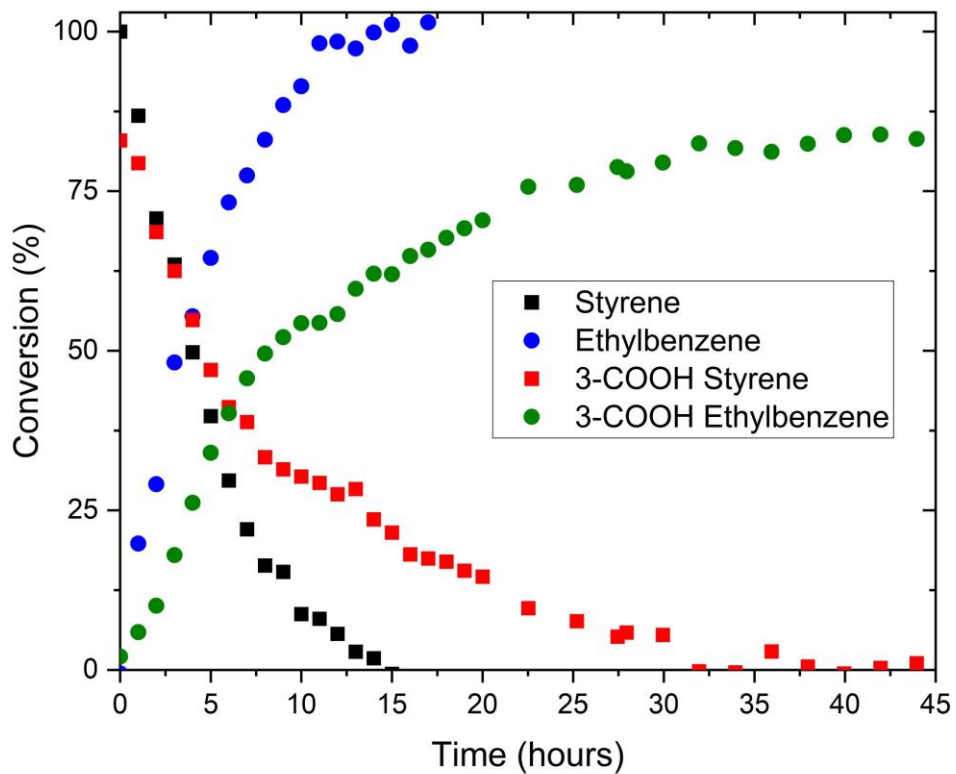


**Figure S56:** Hydrogenation of styrene (black boxes and blue circles) and 3-vinylbenzoic acid + 10 mol% Et<sub>3</sub>N (red boxes and green circles) by Ir-s @ G-sphere\* as two separate experiments. For detailed conditions and procedure, see section above (Catalysis: General procedure of High Pressure NMR experiments).

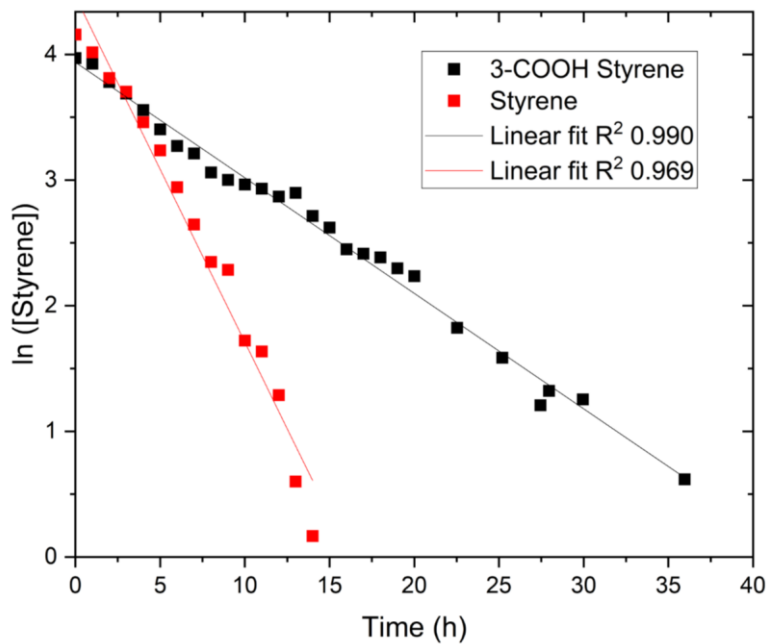


**Figure S57:** First order fit of catalytic hydrogenation experiments of styrene (red boxes) and 3-vinylbenzoic acid + 10 mol% Et<sub>3</sub>N (black boxes) by **Ir-s @ G-sphere\*** as two separate experiments. For detailed conditions and procedure, see section above (Catalysis: General procedure of High Pressure NMR experiments).

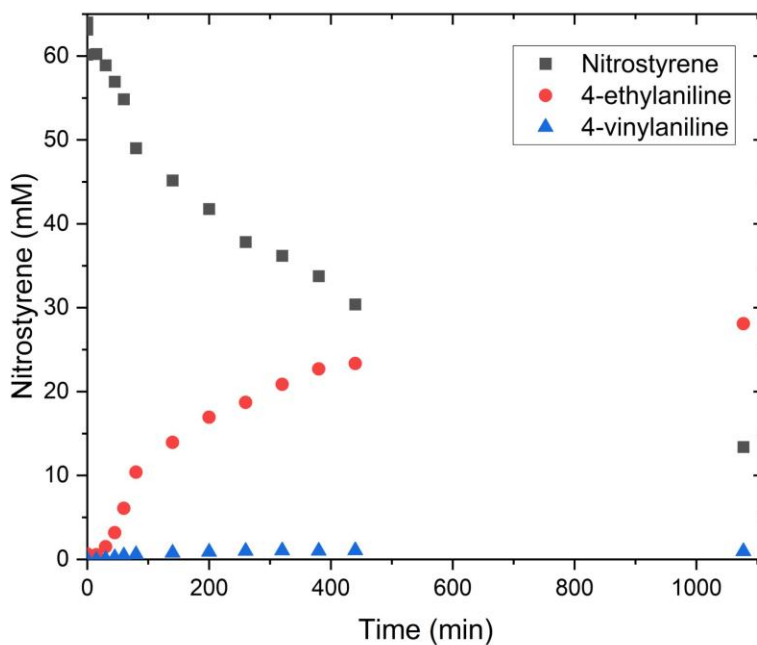
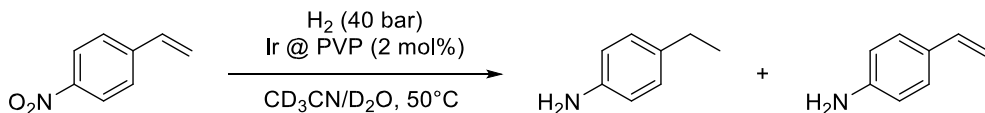


**Figure S58:** Hydrogenation of 4-nitrostyrene by **Ir @ PVP** (2 mol% Ir). For detailed conditions and procedure, see section above (Catalysis: General procedure of High Pressure NMR experiments).

### X-ray photoelectron spectroscopy (XPS)

The solutions of as-prepared **Ir-s @ G-sphere** before and after hydrogenation were drop cast onto a TEM grid (Pure C on Cu grid) and kept under argon atmosphere until transferred to the sample holder for measurement.



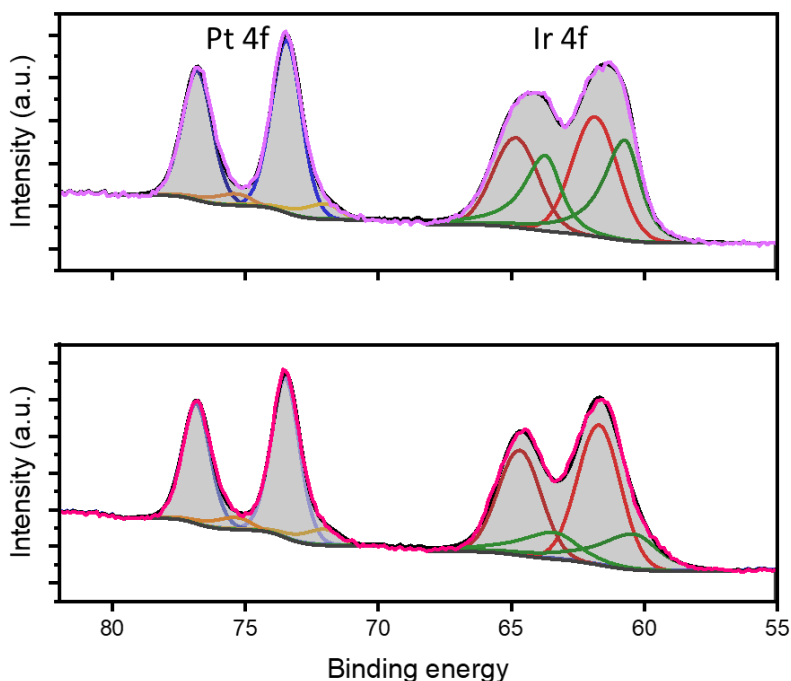


**Figure S59:** XPS images of top: Ir-s @ G-sphere\* (after hydrogenation) and bottom: Ir-s @ G-sphere (before hydrogenation). With the measured spectra (pink/purple), the fitted 4f doublet areas of Ir<sup>I</sup> (red), Ir<sup>0</sup> (green), Pt<sup>II</sup> (blue), Pt<sup>0</sup> (yellow) and the fitted areas combined (black/grey).<sup>16-19</sup>

---

#### Presence of Silver impurities:

Elemental analysis of the encapsulated nanoparticles through EDS mapping (**Figure S60**) and ICP-OES (Table S6) revealed the presence of silver among the Ir nanoclusters. The presence of small quantities of Ag impurities can be traced back to the halide abstraction with AgBF<sub>4</sub> to form Ir-s-BF<sub>4</sub>. Generally, filtration over celite suffices to remove the formed AgCl precipitate. However, in this system containing additional ions (PPh<sub>4</sub><sup>+</sup>, R-SO<sub>3</sub><sup>-</sup>) and a coordinating solvent (CD<sub>3</sub>CN), it can be rationalized that part of the formed silver species may remain solubilized (for example in the form of a AgCl<sub>2</sub>PPh<sub>4</sub> salt or as RSO<sub>3</sub><sup>-</sup>Ag<sup>+</sup>, the former has been identified in MS).

Notably, HAADF-STEM-EDS analysis reveals that the silver content varies per particle (**Figure S60**), in such that small clusters do not display any presence of silver, whereas larger particles contain a sizable amount of silver.

Although these results may suggest that the presence of these silver impurities could have been of influence for some of the larger particles observed, these observations do not affect the key findings of this research. Based on the control experiments (**Ir-s + M-sphere** and **Ir-n + G-sphere**) it is evident that even in the presence of these Ag impurities, supramolecular preorganization within these coordination spheres results in the controlled formation of encapsulated nanoclusters.

To evaluate any effect of Ag impurities on the catalytic performance, we repeated catalytic experiments in the presence of some additional AgBF<sub>4</sub> and compared the outcome to the original system (Table S7). The lack of significant changes in catalytic results suggests that the effect of silver impurities can be deemed negligible.

It should be noted that, although the presence of a silver salt did not affect the catalytic activity, possible alloying during the particle formation process might affect the catalytic outcome. Nonetheless, reports on Ag-Ir alloys extremely remain rare<sup>20</sup> as they are classically known to be poorly miscible. Thus, given possibly limited mixing and the small quantities of silver present in this system, these observed impurities do not affect the main conclusions drawn from these results and further examination of potential alloying would go beyond the scope of the research questions explored in this paper.

Notwithstanding, it will definitely be of interest in future research.

**Table S6:** Found values for ICP-OES measurements of **Ir-s @ G-sphere\*** as prepared and relative mol% of Ir, Pt and Ag.

	<i>mg/ml</i>	<i>mM</i>	<i>Relative mol%</i>
<b>Ir</b>	0.098	0.509	59%
<b>Pt Ag</b>	0.050	0.259	30%
	0.011	0.100	11%

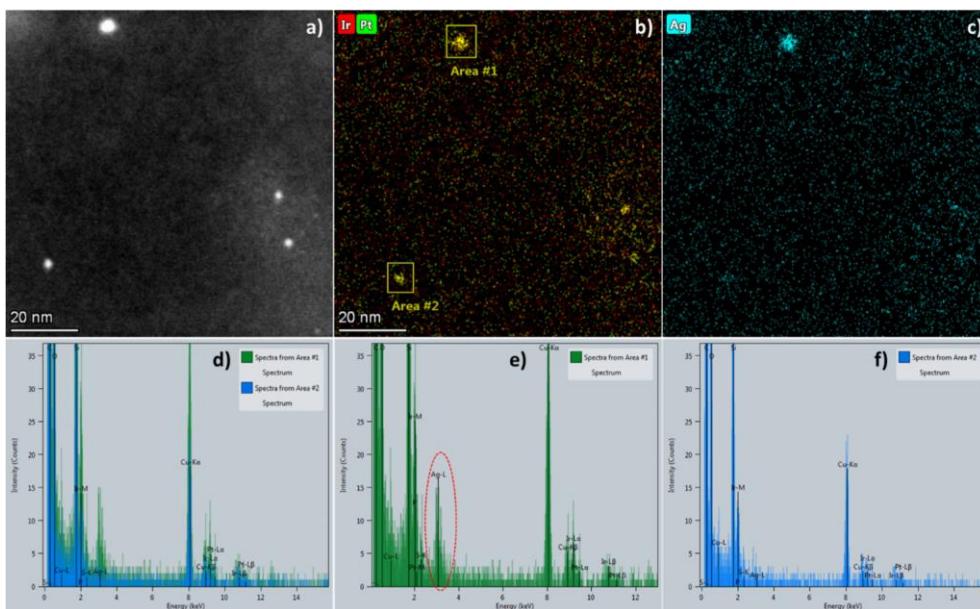


**Figure S60:** a) HAADF-STEM image of **Ir-s@G-sphere\*** and corresponding EDS maps of **b)** an overlay of Ir and Pt and **c)** EDS map of Ag **d)** overlaid EDS patterns of selected areas 1 and 2, and EDS patterns of **e)** area 1 and **f)** area 2.

**Table S7:** Results of catalytic control experiments of 4-nitrostyrene (**1**) hydrogenation with or without additional AgBF<sub>4</sub>. <sup>a)</sup>15mol% AgBF<sub>4</sub> vs **1** <sup>b)</sup> 4.4 mol% AgBF<sub>4</sub> vs **Ir** added before particle synthesis <sup>c)</sup> different reaction conditions: [**1**] = 100 mM in THF, 2% **Ir** vs **1**, vol. = 0.7 ml, 20 bar H<sub>2</sub>, 50°C.

<b>System</b>	<b>Solvent Time Conversion</b>		
<b>G-sphere</b>	CH <sub>3</sub> CN	4h	0%
<b>G-sphere + AgBF<sub>4</sub><sup>a)</sup></b>	CH <sub>3</sub> CN	4h	0%
<b>Ir-s @ G-sphere</b>	CH <sub>3</sub> CN	4h	72%
<b>s @ G-sphere<sup>c)</sup></b>	THF	48h	9%
<sup>a)</sup> <b>Ir-s @ G-sphere + AgBF<sub>4</sub><sup>b,c)</sup></b>	THF	48h	9%
<sup>a)</sup> <b>Ir-s @ G-sphere<sup>c)</sup></b>	THF	92h	45%
<sup>a)</sup> <b>Ir-s @ G-sphere + AgBF<sub>4</sub><sup>b,c)</sup></b>	THF	92h	37%

## EXPERIMENTAL REFERENCES

- 1 D. H. Lee, J. H. Kim, B. H. Jun, H. Kang, J. Park and Y. S. Lee, *Org. Lett.*, 2008, **10**, 1609–1612.
- 2 L. R. Moore, S. M. Cooks, M. S. Anderson, H. J. Schanz, S. T. Griffin, R. D. Rogers, M. C. Kirk and K. H. Shaughnessy, *Organometallics*, 2006, **25**, 5151–5158.
- 3 S. Ahrens, A. Peritz and T. Strassner, *Angew. Chemie Int. Ed.*, 2009, **48**, 7908–7910.

- 4 E. O. Bobylev, D. A. Poole, B. de Bruin and J. N. H. Reek, *Chem. Sci.*, 2021, **12**, 7696–7705.
- 5 O. F. Wendt, N. F. K. Kaiser and L. I. Elding, *J. Chem. Soc. - Dalt. Trans.*, 1997, 4733–4737.
- 6 R. Zaffaroni, E. O. Bobylev, R. Plessius, J. I. Van Der Vlugt and J. N. H. Reek, *J. Am. Chem. Soc.*, 2020, **142**, 8837–8847.
- 7 G. R. Fulmer, A. J. M. Miller, N. H. Sherden, H. E. Gottlieb, A. Nudelman, B. M. Stoltz, J. E. Bercaw and K. I. Goldberg, *Organometallics*, 2010, **29**, 2176–2179.
- 8 M. A. N. Virboul, *Sulfonate Functionalisation of Transition Metal Complexes: A Versatile Tool Towards Catalyst Recovery*, PhD Thesis, Utrecht university, Utrecht, 2011. <https://dspace.library.uu.nl/handle/1874/203778> (accessed 2023-06-01), .
- 9 M. A. N. Virboul, M. Lutz, M. A. Siegler, A. L. Spek, G. Van Koten and R. J. M. Klein Gebbink, *Chem. Eur. J.*, 2009, **15**, 9981–9986.
- 10 M. Bouhrara, E. Jeanneau, L. Veyre, C. Copéret and C. Thieuleux, *Dalt. Trans.*, 2011, **40**, 2995–2999.
- 11 I. Romanenko, D. Gajan, R. Sayah, D. Crozet, E. Jeanneau, C. Lucas, L. Leroux, L. Veyre, A. Lesage, L. Emsley, E. Lacôte and C. Thieuleux, *Angew. Chemie - Int. Ed.*, 2015, **54**, 12937–12941.
- 12 Q. Q. Wang, S. Gonell, S. H. A. M. Leenders, M. Dürr, I. Ivanovic-Burmazovic and J. N. H. Reek, *Nat. Chem.*, 2016, **8**, 225–230.
- 13 E. O. Bobylev, D. A. Poole, B. de Bruin and J. N. H. Reek, *Chem. Eur. J.*, 2021, **27**, 12667–12674.
- 14 M. J. Sharif, P. Maity, S. Yamazoe, T. Tsukuda, *Chem. Lett.* 2013, **42**, 1023–1025.
- 15 D. C. Roe, *J. Magn. Reson.*, 1985, **63**, 388
- 16 H. Y. Hall and P. M. A. Sherwood, *J. Chem. Soc. Faraday Trans. 1 Phys. Chem. Condens. Phases*, 1984, **80**, 135–152.
- 17 C. Crotti, E. Farnetti, S. Filipuzzi, M. Stener, E. Zangrando and P. Moras, *Dalt. Trans.*, 2007, 133–142.
- 18 P. Brant, L. S. Benner and A. L. Balch, *Inorg. Chem.*, 1979, **18**, 3422–3427.
- 19 L. M. Martínez-Prieto, I. Cano, A. Márquez, E. A. Baquero, S. Tricard, L. Cusinato, I. del Rosal, R. Poteau, Y. Coppel, K. Philippot, B. Chaudret, J. Cámpora and P. W. N. M. van Leeuwen, *Chem. Sci.*, 2017, **8**, 2931–2941.
- 20 H. Guo, H. Li, K. Jarvis, H. Wan, P. Kunal, S. G. Dunning, Y. Liu, G. Henkelman and S. M. Humphrey, *ACS Catal.*, 2018, 11386–11397.